

# Mild P–P Bond Cleavage in the Methylidiphosphenyl Complex $[\text{Mo}_2\text{Cp}_2(\mu\text{-PCy}_2)(\mu\text{-}\kappa^2\text{:}\kappa^2\text{-P}_2\text{Me})(\text{CO})_2]$ To Give Novel Phosphide-Bridged Trinuclear Derivatives

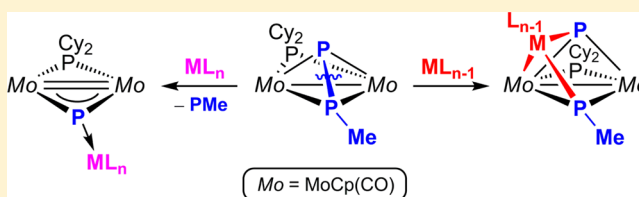
M. Angeles Alvarez,<sup>†</sup> M. Esther García,<sup>†</sup> Daniel García-Vivó,<sup>†</sup> Raquel Lozano,<sup>†</sup> Alberto Ramos,<sup>\*,‡</sup> and Miguel A. Ruiz<sup>\*,‡</sup>

<sup>†</sup>Departamento de Química Orgánica e Inorgánica/IUQOEM, Universidad de Oviedo, E-33071 Oviedo, Spain

<sup>‡</sup>Instituto Nacional del Carbón, Spanish Research Council for Scientific Research (CSIC), Francisco Pintado Fe 26, E-33011 Oviedo, Spain

## Supporting Information

**ABSTRACT:** Reactions of the title diphosphenyl complex with  $[\text{Fe}_2(\text{CO})_9]$  and  $[\text{W}(\text{CO})_4(\text{THF})_2]$  gave the trinuclear species  $[\text{Mo}_2\text{FeCp}_2(\mu_3\text{-P})(\mu\text{-PCy}_2)(\mu_3\text{-PMe})(\text{CO})_5]$  and  $[\text{Mo}_2\text{WCp}_2(\mu_3\text{-P})(\mu\text{-PCy}_2)(\mu_3\text{-PMe})(\text{CO})_6]$  following from formal insertion of the 14-electron fragments  $\text{Fe}(\text{CO})_3$  and  $\text{W}(\text{CO})_4$ , respectively, in the P–P bond of the diphosphenyl ligand and formation of a new heterometallic bond [ $\text{Mo}\text{--}\text{Fe} = 2.9294(6)$  Å and  $\text{Mo}\text{--}\text{W} = 3.146(1)$  Å]. Reactions of the diphosphenyl complex with the tetrahydrofuran adducts  $[\text{ML}_n(\text{THF})]$  ( $\text{ML}_n = \text{MnCp}'(\text{CO})_2, \text{W}(\text{CO})_5$ ) led instead to trinuclear diphosphenyl complexes  $[\text{Mo}_2\text{MCp}_2(\mu\text{-PCy}_2)(\mu_3\text{-}\kappa^2\text{:}\kappa^2\text{-P}_2\text{Me})(\text{CO})_2\text{L}_n]$  following from coordination in each case of the corresponding 16-electron fragment  $\text{ML}_n$  to the lone-pair-bearing P atom of the  $\text{P}_2\text{Me}$  ligand. However, these diphosphenyl complexes were unstable and decomposed at room temperature or under mild heating by the release of methylphosphinidene (PMe), to give the corresponding derivatives  $[\text{Mo}_2\text{MCp}_2(\mu_3\text{-P})(\mu\text{-PCy}_2)(\text{CO})_2\text{L}_n]$  displaying trigonal-planar phosphide ligands, giving rise to strongly deshielded  $^{31}\text{P}$  NMR resonances ( $\delta_{\text{P}}$  ca. 1100 ppm), while being involved in strong  $\pi$  bonding with the unsaturated  $\text{Mo}_2$  center of these molecules [ $\text{Mo}\text{--}\text{Mo} = 2.749(1)$  Å and  $\text{Mo}\text{--}\text{P} = \text{ca. } 2.30$  Å when  $\text{M} = \text{W}$ ]. An isolobal analogy could be established between the  $\text{P}\rightarrow\text{ML}_n$  fragments in these products and a carbyne ligand (CR), supported by density functional theory calculations on the tungsten compound, which also enabled an easy interpretation and prediction of their chemical behavior. Thus, the manganese complex could be reversibly carbonylated ( $p_{\text{CO}} = \text{ca. } 3$  atm, 293 K) to give the corresponding electron-precise pentacarbonyl  $[\text{MnMo}_2\text{Cp}_2\text{Cp}'(\mu_3\text{-P})(\mu\text{-PCy}_2)(\text{CO})_5]$  [ $\text{Mo}\text{--}\text{Mo} = 3.1318(7)$  Å], a process also involving a trans-to-cis rearrangement of the  $\text{Mo}_2\text{Cp}_2$  subunit. On the other hand, decarbonylation of the tungsten complex was accomplished in a refluxing toluene solution to give the hexacarbonyl  $[\text{Mo}_2\text{WCp}_2(\mu_3\text{-P})(\mu\text{-PCy}_2)(\mu\text{-CO})(\text{CO})_5]$ , a derivative containing an unsaturated 30-electron dimolybdenum center with an intermetallic triple bond.



## INTRODUCTION

We recently described the preparation of the methylidiphosphenyl complex  $[\text{Mo}_2\text{Cp}_2(\mu\text{-PCy}_2)(\mu\text{-}\kappa^2\text{:}\kappa^2\text{-P}_2\text{Me})(\text{CO})_2]$  (**1**) through the room-temperature reaction of MeI with the anionic diphosphorus complex  $[\text{Mo}_2\text{Cp}_2(\mu\text{-PCy}_2)(\mu\text{-}\kappa^2\text{:}\kappa^2\text{-P}_2\text{Me})(\text{CO})_2]^-$ , a molecule prepared, in turn, through the symmetrical cleavage of white phosphorus ( $\text{P}_4$ ) by the unsaturated dimolybdenum complex  $[\text{Mo}_2\text{Cp}_2(\mu\text{-PCy}_2)(\mu\text{-CO})_2]^-$  under mild conditions (Scheme 1).<sup>1</sup>

Among the family of reported diphosphenyl complexes, compound **1** represents a unique example of a complex displaying a  $\text{P}_2\text{R}$  ligand symmetrically bridging two metal atoms (type D in Chart 1) because the most common coordination mode for this ligand is the terminal  $\kappa^1$  mode found in mononuclear compounds (type A in Chart 1).<sup>2</sup> There are also some examples of  $\mu_2\text{-P}_2\text{R}$  complexes with other arrangements of the bridging ligand, generally derived from reactions of a parent mononuclear  $\kappa^1$ -diphosphenyl complex with different

metal fragments. Most of these reactions involve the lone pair (LP) of the metal-bound P atom to give a  $\text{P:P}$ -bridged derivative (type B coordination), as found in the reactions of  $[\text{MCp}^*(\text{NO})(\text{CO})(\kappa^1\text{-P}_2\text{Mes}^*)]$  ( $\text{M} = \text{Mn, Re}$ ;  $\text{Mes}^* = 2,4,6\text{-C}_6\text{H}_2\text{tBu}_3$ ) with a  $\text{Cr}(\text{CO})_5$  fragment to give  $[\text{CrMCp}^*(\mu\text{-}\kappa^1\text{:}\kappa^1\text{-P}_2\text{Mes}^*)(\text{NO})(\text{CO})]$ .<sup>3</sup> Alternatively, the terminal complex can bind a second metal fragment through its P–P double bond to give a  $\text{P:P,P}'$ -bridged derivative (type C coordination), as observed in the reaction of  $[\text{FeCp}^*(\text{CO})_2(\kappa^1\text{-P}_2\text{Mes}^*)]$  with a  $\text{Pt}(\text{PPh}_3)_2$  moiety to give  $[\text{FePtCp}^*(\mu\text{-}\kappa^1\text{:}\kappa^2\text{-P}_2\text{Mes}^*)(\text{CO})_2(\text{PPh}_3)_2]$ .<sup>4</sup> Finally, a few examples of the  $\mu_3\text{-P}_2\text{R}$  complexes have been also reported, these involving the participation of both P-based LPs and also the P–P double bond for binding to the metal atoms, as found in the triiron complexes  $[\text{Fe}_3\text{Cp}_3(\text{CO})_2(\mu_3\text{-}\kappa^1\text{:}\kappa^2\text{-P}_2\text{tBu})(\mu_3\text{-P}^t\text{Bu})]$  (type

Received: July 30, 2014

Published: October 10, 2014

Scheme 1

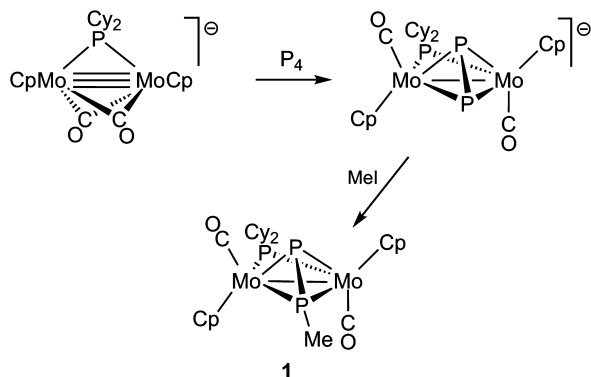
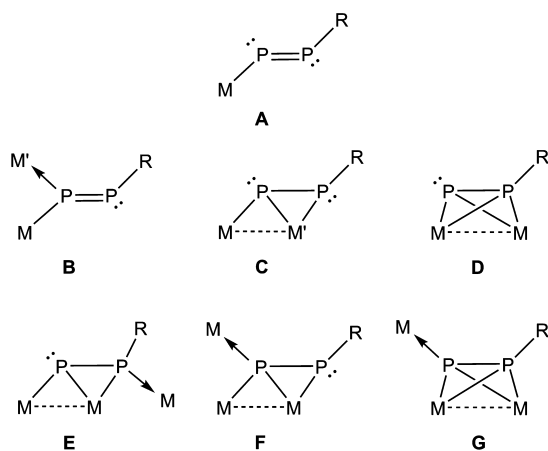


Chart 1



E),<sup>5</sup>  $[\text{Fe}_3\text{Cp}^*(\mu_3\text{-}\kappa^1\text{:}\kappa^1\text{:}\kappa^2\text{-P}_2\text{tBu})(\text{CO})_{10}]$  (type F),<sup>6</sup> and  $[\text{Fe}_3\text{Cp}^*(\mu_3\text{-}\kappa^1\text{:}\kappa^2\text{:}\kappa^2\text{-P}_2\text{tBu})(\text{CO})_8]$  (type G).<sup>6</sup>

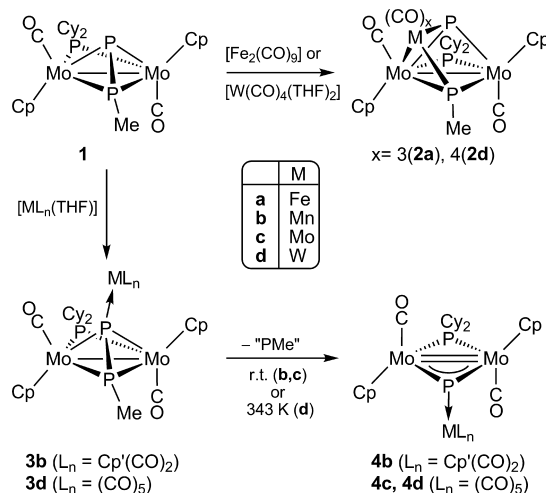
Complexes of types F and G can obviously be related to those of types C and D, respectively, and expected to be formed from the latter ones upon additional coordination of a 16-electron metal fragment through the LP at the bridgehead P atom. Unfortunately, the behavior of complexes with bridging diphosphenyl ligands has been little explored to date, and the outcome of these seemingly simple reactions might not be so straightforward. In particular, reactions of a type D diphosphenyl complex with an unsaturated metal fragment might involve P–P cleavage (or insertion) processes. Precedents for such possible outcomes can be found in the reaction of the  $\mu_3$ -diphosphenyl complex  $[\text{Fe}_3\text{Cp}^*(\mu_3\text{-}\kappa^2\text{:}\kappa^2\text{:}\kappa^1\text{-P}_2\text{tBu})(\text{CO})_8]$  with  $[\text{Fe}_2(\text{CO})_9]$  to give  $[\text{Fe}_3\text{Cp}^*\{\mu_3\text{-}\kappa^2\text{:}\kappa^2\text{:}\kappa^1\text{-PC(O)P}^t\text{Bu}\}(\text{CO})_8]$ , with the latter following from insertion of a CO molecule in the P–P bond of the diphosphenyl ligand,<sup>6</sup> and in the room temperature reaction of the diphosphorus-bridged complex  $[\text{Re}_2\text{Cp}^*_2(\mu\text{-}\kappa^2\text{:}\kappa^2\text{-P}_2)(\text{CO})_4]$  (a molecule related to diphosphenyl complexes of type D) with  $[\text{W}(\text{CO})_5(\text{THF})]$  (THF = tetrahydrofuran) to give inter alia a phosphide complex  $[\text{W}_2\text{Re}_2\text{Cp}^*_2(\mu_3\text{-P})_2(\text{CO})_{12}]$  derived from insertion of the tungsten fragment in the P–P bond of the diphosphorus ligand.<sup>7</sup> Because cleavage of P–P bonds in this sort of ligand is a matter of general interest in the context of  $\text{P}_4$  activation by transition-metal complexes<sup>8</sup> and recalling that eventually compound **1** is derived itself from white phosphorus, we considered it of interest to explore the reactivity of our diphosphenyl complex with different precursors of 14- and 16-electron metal carbonyl fragments. These reactions, however,

proved to be rather complex and strongly dependent on the stoichiometry and reaction conditions, and we here report on those reactions incorporating a single metal fragment, while those leading to tetranuclear derivatives of **1** will be reported separately.<sup>9</sup> As will be shown below, all reactions incorporating a single metal fragment eventually involve the cleavage of the P–P bond in the diphosphenyl ligand of **1** under mild conditions, to yield derivatives containing phosphide and methylphosphinidene ligands, with the latter being sometimes decoordinates along the process.

## RESULTS AND DISCUSSION

**Incorporation of 14-Electron Metal Fragments.** Compound **1** reacted readily at room temperature with stoichiometric amounts of  $[\text{Fe}_2(\text{CO})_9]$  to give the trinuclear phosphide methylphosphinidene complex  $[\text{Mo}_2\text{FeCp}_2(\mu_3\text{-P})(\mu\text{-PCy}_2)(\mu_3\text{-PMe})(\text{CO})_5]$  (**2a**), formally derived from addition of the 14-electron fragment  $\text{Fe}(\text{CO})_3$  to a  $\text{MoP}_2$  face of the  $\text{Mo}_2\text{P}_2$  tetrahedral core of **1** with full scission of the P–P bond (Scheme 2). Analogously, reaction of **1** with a freshly prepared

Scheme 2



solution of the THF adduct  $[\text{W}(\text{CO})_4(\text{THF})_2]$  gave  $[\text{Mo}_2\text{WCp}_2(\mu_3\text{-P})(\mu\text{-PCy}_2)(\mu_3\text{-PMe})(\text{CO})_6]$  (**2d**), a trinuclear cluster displaying a structure comparable to that of **2a**, as discussed below, and following analogously from formal addition of the 14-electron fragment  $\text{W}(\text{CO})_4$  to a  $\text{MoP}_2$  face of the core of **1** with P–P bond cleavage. This reaction, however, also gave small amounts of the type G diphosphenyl complex  $[\text{Mo}_2\text{WCp}_2(\mu\text{-PCy}_2)(\mu_3\text{-}\kappa^2\text{:}\kappa^2\text{-P}_2\text{Me})(\text{CO})_7]$  (**3d**) and the phosphide derivative  $[\text{Mo}_2\text{WCp}_2(\mu_3\text{-P})(\mu\text{-PCy}_2)(\text{CO})_7]$  (**4d**). The latter side products contain  $\text{W}(\text{CO})_5$  fragments and likely are derived from the presence of small amounts of the pentacarbonyl adduct  $[\text{W}(\text{CO})_5(\text{THF})]$  in the corresponding reaction mixtures, as shown by separate experiments to be discussed later on (Scheme 2). On the other hand, we note that formation of the pentacarbonyl complex **2a** is itself somewhat unexpected because  $[\text{Fe}_2(\text{CO})_9]$  is a well-known precursor of the 16-electron fragment  $\text{Fe}(\text{CO})_4$  and is therefore expected to lead to a type G derivative, as noted above. It is likely that such a derivative might be initially formed in the above reaction and then rapidly undergoes decarbonylation to yield **2a**, a matter to be discussed in more detail later on.

**Solid-State Structure of Compounds 2a and 2d.** The structure of 2a in the crystal lattice (Figure 1 and Table 1) can

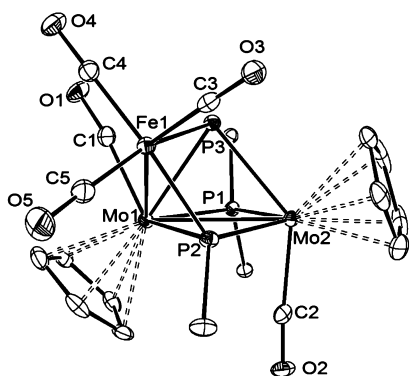


**Figure 1.** ORTEP diagram (30% probability) of compound 2a with H atoms and Cy groups (except the C1 atoms) omitted for clarity.

**Table 1.** Selected Bond Lengths (Å) and Angles (deg) for Compound 2a

Mo1–Mo2	2.9897(4)	C1–Mo1–Mo2	116.2(1)
Mo1–Fe1	2.9294(6)	C2–Mo2–Mo1	83.5(1)
Mo1–P1	2.4852(8)	P3–Mo1–P1	73.79(3)
Mo2–P1	2.4289(8)	P3–Mo2–P1	74.11(3)
Mo1–P2	2.4565(9)	P2–Mo1–P1	101.91(3)
Mo2–P2	2.3665(9)	P2–Mo2–P1	106.32(3)
Mo1–P3	2.4769(9)	P2–Mo1–P3	65.60(3)
Mo2–P3	2.5133(9)	P2–Mo2–P3	66.33(3)
Fe1–P2	2.176(1)	P2–Fe1–P3	73.10(3)
Fe1–P3	2.308(1)	Mo1–Fe1–P3	54.91(2)
Mo1–C1	1.965(4)	Mo1–Fe1–P2	55.17(3)
Mo2–C2	1.983(4)	C3–Fe1–C4	99.1(2)
Fe1–C3	1.766(4)	C3–Fe1–C5	102.6(2)
Fe1–C4	1.812(4)	C4–Fe1–C5	95.1(2)
Fe1–C5	1.785(4)		
P2–C6	1.859(4)		

be derived from that of the parent methylphosphinidene complex **1** after addition of a pyramidal  $\text{Fe}(\text{CO})_3$  fragment to the  $\text{Mo1-P2-P3}$  face of the tetrahedral  $\text{Mo}_2\text{P}_2$  core of **1** with full cleavage of the P–P bond, as indicated by the long P–P separation of 2.672(1) Å [cf. 2.085(1) Å in **1**],<sup>2</sup> thus giving rise to new phosphinidene (PMe) and phosphide (P) ligands, both of them triply bridging the resulting V-shaped  $\text{Mo}_2\text{Fe}$  metal core. The somewhat distorted transoid arrangement of the molybdenum-bound Cp and CO ligands, denoted by the quite different Mo–Mo–CO angles of 116.2(1) and 83.5(1)°, is reminiscent of that found in the parent complex **1** and related derivatives of the anion  $[\text{Mo}_2\text{Cp}_2(\mu\text{-PCy}_2)(\mu\text{-}\kappa^2\text{-}\kappa^2\text{-P}_2)(\text{CO})_2]^-$ ,<sup>1,10</sup> probably caused here by the steric pressure induced by the apical P atom (P3) and the  $\text{Fe}(\text{CO})_3$  fragment on the CO ligand attached to Mo1, while the basal P atom (P2) remains placed close to the  $\text{Mo}_2\text{P}(\text{Cy})$  plane. The Mo–Mo bond distance of 2.9897(4) Å is consistent with the formulation of a single Mo–Mo bond, as required on the basis of the 18-electron rule for this molecule, and the same can be said of the Mo1–Fe1 separation of 2.9294(6) Å, which is comparable to that measured for the 34-electron complex  $[\text{FeMoCp}(\mu\text{-PCy}_2)(\text{CO})_6]$ .<sup>11</sup>

The coordination of phosphide and methylphosphinidene ligands in **2a** deserves some comments. As for the first ligand,

we note that most pyramidal  $\mu_3\text{-P}$  complexes structurally characterized so far involve P atoms bridging metal triangles, and compounds **2a** and **2d** actually represent the first examples of V-shaped trinuclear clusters triply bridged by a phosphide ligand to be structurally characterized. The Mo–P3 separations of 2.50 Å are only slightly shorter than the corresponding separations in **1** (ca. 2.53 Å), while the Fe–P3 length [2.308(1) Å] is ca. 0.2 Å shorter, as expected from the difference in covalent radii of Mo and Fe atoms.<sup>12</sup> These separations are thus consistent with a formal description of the P atom as contributing with one electron to each of the metal atoms. For comparison, the phosphide ligands bridging triangular faces in the clusters  $[\text{W}_6\text{Cp}^*_2(\mu_3\text{-P})_2(\mu_4\text{-P})_2(\text{CO})_{16}]^{13}$  and  $[\text{Mo}_2\text{WCp}_2\text{Cp}^*(\mu_3\text{-P})(\text{CO})_6]^{14}$  display M–P lengths in the range 2.39–2.52 Å.

In order to fulfill an 18-electron configuration around each metal center, however, the phosphinidene ligand should contribute with one electron to each Mo atom and with two electrons to the Fe atom. This is in agreement with the quite short Fe1–P2 length of 2.176(1) Å, which falls in the range of distances found for compounds of the formula  $[\text{Fe}_2\text{Cp}_2(\mu\text{-CO})_2(\text{CO})(\text{PR}_3)]$  (2.13–2.21 Å) having classical two-electron P-atom donors.<sup>15</sup> Moreover, it might be anticipated that the lower coordination number of the Mo2 atom should be balanced with a stronger coordination of the  $\text{PCy}_2$  ligand to that center, which is in agreement with the shorter P1–Mo2 length of 2.4289(8) Å [cf. 2.4852(8) Å for P1–Mo1], although the phosphinidene ligand also seems involved in the task because it is also placed significantly closer to the Mo2 atom [2.3665(9) vs 2.4565(9) Å]. We finally note the coordination environment of the phosphinidene P atom in **2a**, with the methyl group almost placed in the Fe1–P2–Mo2 plane, thus configuring a geometry strongly departing from the more common tetrahedral environment of phosphorus. This geometry likely allows for a stronger interaction of phosphorus with the Fe1 and Mo2 atoms (recall the shorter lengths of these bonds), and is not unusual in 50-electron (hence V-shaped) trinuclear clusters bridged by phosphinidene ligands,<sup>16</sup> although it seems that no related clusters containing group 6 metals have been structurally characterized so far.

The structure of **2d** in the crystal lattice is comparable to that of **2a** if we just replace the  $\text{Fe}(\text{CO})_3$  fragment with the isoelectronic  $\text{W}(\text{CO})_4$  one; therefore, a detailed discussion is not needed. There are two independent molecules in the unit cell, quite similar to each other, and a view emphasizing the V-shaped metal core of one of the two molecules is shown in Figure 2, while the most relevant geometrical parameters are collected in Table 2. As found for the iron cluster, the  $\text{PCy}_2$  and PMe ligands are placed ca. 0.1 Å closer to the Mo atom having the lower coordination number (Mo1 here), and the phosphinidene ligand formally provides the W atom with two electrons, in agreement with the very short W–P2 length of 2.409(1) Å [cf. 2.594(1) Å for W–P1]. The newly formed Mo–W bond [3.146(1) Å] is longer than the  $\text{PCy}_2$ -bridged Mo–Mo bond [2.976(1) Å], but such an intermetallic length still is fairly normal for a single bond. For comparison, the phosphinidene-bridged Mo–Mo bonds in the 48-electron clusters  $[\text{Mo}_2\text{MCp}_2(\mu_3\text{-PPh})(\text{CO})_7]$  (M = Fe, Ru) display comparable Mo–Mo lengths of ca. 3.17 Å.<sup>17</sup>

**Solution Structure of Compounds 2a and 2d.** The IR spectrum of compound **2a** in a dichloromethane solution exhibits four CO stretching bands at 2010, 1945, 1927, and 1892  $\text{cm}^{-1}$  (Table 3). The first three bands can be attributed to



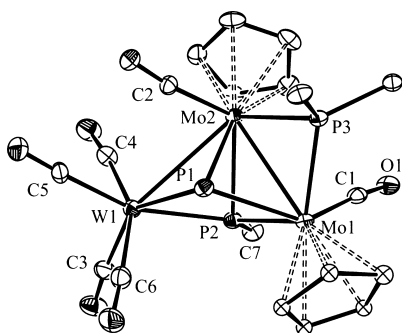


**Figure 2.** ORTEP diagram (30% probability) of one of the two independent molecules of compound **2d** in the unit cell, with H atoms and Cy groups (except the C1 atoms) omitted for clarity.

**Table 2.** Selected Bond Lengths (Å) and Angles (deg) for Compound **2d**

Mo1–Mo2	2.976(1)	C1–Mo1–Mo2	83.6(2)
Mo2–W1	3.146(1)	C2–Mo2–Mo1	117.5(1)
Mo1–P1	2.492(2)	P3–Mo1–P1	73.34(5)
Mo2–P1	2.452(1)	P3–Mo2–P1	72.51(4)
Mo1–P2	2.399(1)	P2–Mo1–P1	69.13(5)
Mo2–P2	2.526(1)	P2–Mo2–P1	67.75(5)
Mo1–P3	2.413(1)	P2–Mo1–P3	108.70(5)
Mo2–P3	2.501(1)	P2–Mo2–P3	102.08(4)
W1–P1	2.594(1)	P1–W1–P2	67.29(5)
W1–P2	2.409(1)	W1–P1–Mo1	106.18(5)
Mo1–C1	1.979(5)	W1–P1–Mo2	77.10(4)
Mo2–C2	1.993(5)	W1–P2–Mo1	115.53(5)
W1–C3	1.993(5)	W1–P2–Mo2	79.18(4)
W1–C4	2.042(5)	C3–W1–C4	83.5(2)
W1–C5	2.007(5)	C4–W1–C5	81.5(2)
W1–C6	2.021(5)	C3–W1–C5	107.7(2)
P2–C7	1.851(5)		

a pyramidal  $\text{Fe}(\text{CO})_3$  oscillator in a low-symmetry environment<sup>18</sup> and are comparable to those measured in the related clusters  $[\text{FeMo}_2\text{Cp}_2(\mu_3\text{-X})(\mu\text{-PCy}_2)(\text{CO})_5]$  ( $\text{X} = \text{COMe}$ ,  $\text{OMe}$ ),<sup>19</sup> or  $[\text{FeMo}_2\text{Cp}_2(\mu\text{-PPH}_2)(\mu_3\text{-CCPh})(\text{CO})_5]$ .<sup>20</sup> The fourth band can be attributed to the  $\text{Mo}_2(\text{CO})_2$  oscillator of the molecule, but the other band arising from this fragment cannot be identified in solution. This circumstance is not unusual in heterometallic clusters combining  $\text{Mo}_2(\text{CO})_2$  oscillators with  $\text{M}(\text{CO})_x$  ones ( $x = 3\text{--}5$ ) and is due to the comparatively low intensity of the bands mainly arising from

the former oscillator.<sup>19</sup> In fact, the IR spectrum of **2a** recorded in a Nujol mull allows identification of the two bands assignable to the  $\text{Mo}_2(\text{CO})_2$  fragment, which appear at 1868 (m) and 1829 (w, sh)  $\text{cm}^{-1}$ , in positions comparable to those of several heterometallic derivatives of the type  $[\text{Mo}_2\text{MCp}_2(\mu\text{-PCy}_2)(\mu_3\text{-}\kappa^2\text{:}\kappa^2\text{:}\kappa^1\text{-P}_2)(\text{CO})_2\text{L}_n]$  having structures comparable to that of **1**.<sup>10</sup> In the same line, we note that the IR spectrum of **2d** in solution exhibits only two bands of strong intensity at 2010 and 1911  $\text{cm}^{-1}$ , which are clearly assignable to the C–O stretches of the  $\text{W}(\text{CO})_4$  fragment, while no bands at frequencies below 1900  $\text{cm}^{-1}$  attributable to the  $\text{Mo}_2(\text{CO})_2$  oscillator are observed in this case.

The NMR spectra of compounds **2a** and **2d** are essentially consistent with their solid-state structures. The  $^{31}\text{P}\{^1\text{H}\}$  NMR spectra show in each case three distinct resonances corresponding to the PMe, P, and  $\text{PCy}_2$  ligands, respectively (Table 3). The phosphide and phosphinidene ligands display negligible mutual coupling, in agreement with the P–P bond cleavage operated on the former diphosphenyl ligand (cf.  $^1J_{\text{PP}} = 503$  Hz in **1**), and the  $\text{PCy}_2$  ligand in **2a** displays moderate but distinct two-bond coupling to the PMe (14 Hz) and P (9 Hz) ligands, which are close to zero in the case of **2d**. The  $^{31}\text{P}$  chemical shifts of ca. 300 ppm for the PMe ligands in **2a** and **2d** are not very unusual for phosphinidene ligands bridging three metal atoms,<sup>16,21,22</sup> but the shifts of 239.2 and 124.5 ppm for the phosphide ligands in these clusters must be considered as rather low for a pyramidal  $\mu_3\text{-P}$  ligand. For comparison, the phosphide bridging the trimetal core in the 48-electron clusters  $[\text{Mo}_2\text{MCp}_3(\mu_3\text{-P})(\text{CO})_6]$  displays chemical shifts of 560.3 and 459.0 ppm when  $\text{M} = \text{Mo}$  and  $\text{W}$ , respectively.<sup>23</sup> Such relative shieldings in compounds **2** are likely derived from the fact that these molecules are V-shaped, 50-electron clusters rather than triangular, 48-electron clusters, and we notice that a similar shielding effect has been previously found for phosphinidene-bridged trinuclear clusters when going from 48- to 52-electron species.<sup>16,22</sup> We finally note that the  $^1\text{H}$  and  $^{13}\text{C}\{^1\text{H}\}$  NMR spectra of these compounds are generally consistent with the absence of any symmetry element in these molecules, except for the  $^{13}\text{C}$  resonances of the heterometallic  $\text{M}(\text{CO})_n$  fragment, which in both cases appear as just a single resonance at 212.8 (Fe) or 215.9 (W) ppm. This is indicative of the operation in solution of a dynamic process fast on the NMR time scale, not investigated but likely involving the pyramidal rotation of the  $\text{M}(\text{CO})_n$  fragment to render time-averaged equivalence for all CO ligands in the fragment.

**Table 3.** Selected IR<sup>a</sup> and  $^{31}\text{P}\{^1\text{H}\}$  NMR Data<sup>b</sup> for New Compounds

compound	$\nu(\text{CO})$	$\delta_{\text{P}} (J_{\text{PP}}) [J_{\text{PW}}]$		
		$\text{PCy}_2$	P	PMe
$[\text{Mo}_2\text{FeCp}_2(\mu_3\text{-P})(\mu\text{-PCy}_2)(\mu_3\text{-PMe})(\text{CO})_5]$ ( <b>2a</b> )	2010 (vs), 1945 (m), 1927 (m), 1892 (m)	151.4 (14, 9)	239.2 (9)	268.2 (14)
$[\text{Mo}_2\text{WCp}_2(\mu_3\text{-P})(\mu\text{-PCy}_2)(\mu_3\text{-PMe})(\text{CO})_6]$ ( <b>2d</b> )	2010 (vs), 1911 (vs)	165.7 (br)	124.5 (br)	321.5 (br)
$[\text{MnMo}_2\text{Cp}_2\text{Cp}'(\mu\text{-PCy}_2)(\mu_3\text{-P}_2\text{Me})(\text{CO})_4]$ ( <b>3b</b> )		157.4 (br) <sup>c</sup>	–42.9 (br, 400) <sup>c</sup>	–180.3 (br, 400) <sup>c</sup>
$[\text{Mo}_2\text{WCp}_2(\mu\text{-PCy}_2)(\mu_3\text{-P}_2\text{Me})(\text{CO})_7]$ ( <b>3d</b> )	2065 (w), 1938 (vs), 1918 (m, sh) <sup>d</sup>	148.7 (56, 16) <sup>e</sup>	–236.7 (419, 56) <sup>e</sup>	–154.9 (419, 16) <sup>e</sup>
$[\text{Mo}_2\text{Cp}_2\text{Cp}'(\mu_3\text{-P})(\mu\text{-PCy}_2)(\text{CO})_4]$ ( <b>4b</b> )	1941 (s), 1885 (vs)	117.6	1103.3	
$[\text{Mo}_3\text{Cp}_2(\mu_3\text{-P})(\mu\text{-PCy}_2)(\text{CO})_7]$ ( <b>4c</b> )	2064 (m), 1947 (vs)	124.7	1159.3	
$[\text{Mo}_2\text{WCp}_2(\mu_3\text{-P})(\mu\text{-PCy}_2)(\text{CO})_7]$ ( <b>4d</b> )	2062 (m), 1942 (vs)	126.8	1081.4 [156]	
$[\text{MnMo}_2\text{Cp}_2\text{Cp}'(\mu_3\text{-P})(\mu\text{-PCy}_2)(\text{CO})_5]$ ( <b>5</b> )	1964 (s), 1924 (vs), 1889 (s), 1859 (s)	223.2 (11)	951.0 (11)	
$[\text{Mo}_2\text{WCp}_2(\mu_3\text{-P})(\mu\text{-PCy}_2)(\mu\text{-CO})(\text{CO})_5]$ ( <b>6</b> )	2063 (m), 1941 (vs), 1714 (w)	246.0 (30)	925.2 (30) [160]	

<sup>a</sup>Recorded in a dichloromethane solution, with CO stretching bands [ $\nu(\text{CO})$ ] in  $\text{cm}^{-1}$ . <sup>b</sup>Recorded in  $\text{CD}_2\text{Cl}_2$  at 121.50 MHz and 298 K, with coupling constants [ $J_{\text{PP}}$ ] and [ $J_{\text{PW}}$ ] in hertz. <sup>c</sup>In THF at 162.14 MHz. <sup>d</sup>In toluene. <sup>e</sup>In toluene at 162.14 MHz.

**Incorporation of 16-Electron Metal Fragments.** Reactions of **1** with the metal carbonyl adducts  $[\text{MnCp}'(\text{CO})_2(\text{THF})]$  and  $[\text{W}(\text{CO})_5(\text{THF})]$  at room temperature yielded the expected trinuclear complexes  $[\text{MnMo}_2\text{Cp}_2\text{Cp}'(\mu\text{-PCy}_2)(\mu_3\text{-}\kappa^2\text{:}\kappa^2\text{:}\kappa^1\text{-P}_2\text{Me})(\text{CO})_4]$  (**3b**) and  $[\text{Mo}_2\text{WCp}_2(\mu\text{-PCy}_2)(\mu_3\text{-}\kappa^2\text{:}\kappa^2\text{:}\kappa^1\text{-P}_2\text{Me})(\text{CO})_7]$  (**3d**) following from addition of the corresponding 16-electron metal fragments via the LP of the apical P atom of the diphosphenyl ligand (Scheme 2;  $\text{Cp}' = \eta^5\text{-C}_5\text{H}_4\text{Me}$ ). However, these compounds turned out to be rather unstable and could only be characterized partially in solution by IR and NMR inspection of the crude reaction mixtures, which progressively evolve to give the corresponding phosphide complexes  $[\text{MnMo}_2\text{Cp}_2\text{Cp}'(\mu_3\text{-P})(\mu\text{-PCy}_2)(\text{CO})_4]$  (**4b**) and  $[\text{Mo}_2\text{WCp}_2(\mu_3\text{-P})(\mu\text{-PCy}_2)(\text{CO})_7]$  (**4d**). The tungsten compound **3d** was thermally more robust, and full transformation into **4d** was more conveniently completed upon stirring a toluene solution of the complex at 343 K for 2 h. However, we noticed that both transformations **3a,3d/4a,4d** occur very rapidly upon attempted chromatographic purification on alumina even at 253 K. We finally note that compounds **4** follow from formal loss of methylphosphinidene in the diphosphenyl complexes **3**, but the fate of this unstable molecule could not be determined because no major resonances other than those attributed to compounds **4b** and **4d** were present in the  $^{31}\text{P}$  NMR spectra of the corresponding reaction mixtures.

Reaction of compound **1** with the related THF adduct  $[\text{Mo}(\text{CO})_5(\text{THF})]$  is more complex because it gives initially three different products that we have only identified through the  $^{31}\text{P}$  NMR spectra of the crude reaction mixture. These uncharacterized substances (denoted as A–C; see the Experimental Section) decompose rapidly during attempted purification to give the phosphide derivative  $[\text{Mo}_3\text{Cp}_2(\mu_3\text{-P})(\mu\text{-PCy}_2)(\text{CO})_7]$  (**4c**) as the unique product. Because the latter is isolated in good yield after chromatographic workup (ca. 75%), we suggest that all three species eventually decompose to give the same phosphide derivative **4c**. Although we have not characterized these intermediates, it is obvious that they still preserve the PMe moiety because they all display three distinct  $^{31}\text{P}$  NMR resonances. However, the connectivity between the P atoms of the former diphosphenyl ligand could not be unambiguously determined in compounds A–C because they all exhibited moderate P–P couplings in the range 80–100 Hz, thus ruling out a type G coordination of this ligand comparable to that observed in compounds **3**, characterized by much larger one-bond couplings (ca. 400 Hz). In any case, our results indicate that the  $\kappa^2\text{:}\kappa^2\text{:}\kappa^1$ -coordination mode of the diphosphenyl ligand in these systems (type G in Chart 1) is somehow disfavored, a matter to be discussed later on.

**Solid-State and Electronic Structure of 4d.** The structure of this phosphide-bridged complex was confirmed through a single-crystal X-ray diffraction analysis (Figure 3 and Table 4). Although there is some disorder reducing the quality of data (see the Experimental Section), the essential structural features are well-defined. The molecule is built from two  $\text{MoCp}(\text{CO})$  fragments arranged in a transoid fashion and symmetrically bridged by a  $\text{PCy}_2$  ligand and by a trigonal-planar phosphide ligand (P1), which is also bound to an exocyclic  $\text{W}(\text{CO})_5$  moiety, thus completing an octahedral coordination environment around the W atom. The Mo atoms are likely connected through a double bond, as suggested by the short intermetallic separation of 2.749(2) Å, which is only marginally

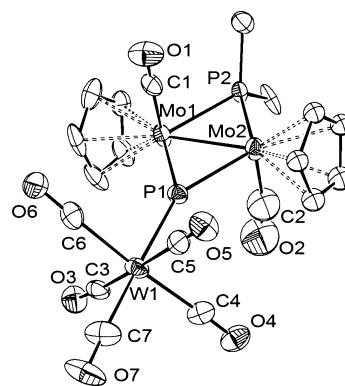


**Figure 3.** ORTEP diagram (30% probability) of compound **4d** with H atoms and Cy groups (except the C1 atoms) omitted for clarity.

**Table 4.** Selected Bond Lengths (Å) and Angles (deg) for Compound **4d**

Mo1–Mo2	2.749(2)	P2–Mo1–P1	107.8(1)
Mo1–P1	2.305(4)	P2–Mo2–P1	109.0(1)
Mo2–P1	2.302(4)	Mo1–P1–Mo2	73.3(1)
Mo1–P2	2.417(3)	Mo1–P2–Mo2	69.9(1)
Mo2–P2	2.383(3)	C1–Mo1–Mo2	79.1(5)
P1–W1	2.457(3)	C2–Mo2–Mo1	84.6(8)
Mo1–C1	2.04(2)	Mo1–P1–W1	144.4(2)
Mo2–C2	2.00(2)	Mo2–P1–W1	142.4(2)
W1–C3	2.01(2)	P1–W1–C3	90.5(4)
W1–C4	2.03(2)	P1–W1–C4	87.1(5)
W1–C5	2.06(2)	P1–W1–C5	89.6(4)
W1–C6	2.06(2)	P1–W1–C6	87.1(5)
W1–C7	2.03(2)	P1–W1–C7	178.1(7)

longer than the one determined for the related 32-electron diphenylphosphide complex  $[\text{Mo}_2\text{Cp}_2(\mu\text{-PPh}_2)_2(\text{CO})_2]$  (ca. 2.71 Å).<sup>24</sup> As found for the latter molecule, the planar  $\text{Mo}_2\text{P}_2$  core is nearly perpendicular to the average plane defined by the Mo atoms and the carbonyl ligands attached to them ( $\text{C1–Mo1–Mo2–P1} = \text{ca. } 88^\circ$ ), while the latter ligands are leaning over the Mo–Mo vector ( $\text{Mo–Mo–CO} = \text{ca. } 80^\circ$ ). These structural features are characteristic of all unsaturated complexes of the type  $[\text{Mo}_2\text{Cp}_2(\mu\text{-PCy}_2)(\mu\text{-X})(\text{CO})_2]$  ( $\text{X} = \text{H, R, CR, COR, NCHR}$ ) previously described by us.<sup>25</sup>

Analysis of the binding in the trigonal-planar  $[\Sigma(\text{M–P1–M}') = \text{ca. } 360^\circ]$  phosphide ligand of **4d** is less straightforward. There are some 10 complexes with this geometry around phosphorus structurally characterized so far. Among them, those involving Mo or W atoms display quite diverse M–P lengths, in the range 2.27–2.54 Å, obviously following from accommodation of the phosphide ligand to different electronic demands of the metal fragments bound to it. In the case of **4d**, the Mo–P lengths of ca. 2.30 Å are ca. 0.1 Å shorter than the corresponding lengths for the  $\text{PCy}_2$  ligand and therefore indicative of substantial multiplicity in these bonds. Actually, these lengths are almost identical with those measured for the phosphinidene-bridged complexes  $[\text{Mo}_2\text{Cp}_2(\mu\text{-PMes}^*)(\text{CO})_4]$ ,<sup>26</sup>  $[\text{Mo}_2\text{Cp}_2\text{I}_2(\mu\text{-PMes}^*)(\text{CO})_2]$ ,<sup>27</sup> and  $[\text{Mo}_2\text{Cp}_2(\mu\text{-PMes}^*)(\mu\text{-CO})_2]$ ,<sup>28</sup> which also display trigonal-planar environments around the P atom, with formal Mo–P bond orders of 1.5,<sup>29,30</sup> while the formal intermetallic bond orders increase from 1 to 3 along this series. The  $\text{W1–P1}$  distance of 2.457(3) Å in **4d** can be considered as consistent with a description of the corresponding interaction as a dative  $\text{P} \rightarrow \text{W}$  bond. The

obvious metric references in this case are mononuclear phosphine compounds of the type  $[\text{W}(\text{CO})_5(\text{PR}_3)]$ , but an inspection of the (many) available structures in the Cambridge Crystallographic Database revealed that these distances are considerably influenced by the steric demands of the R groups. In the absence of strong steric repulsions, these W–P lengths are usually found slightly below 2.50 Å, reaching values as short as 2.45 Å for some cyclic phosphines<sup>31</sup> or even ca. 2.38 Å for cyclic phosphites.<sup>32</sup>

The above geometric analysis supports our view of the P–W interaction in **4d** as a dative single bond, while  $\pi$  bonding of the phosphide ligand would mainly involve the Mo atoms. A similar situation has been previously found in the alkoxide complexes  $[\text{W}_4(\text{OR})_4(\mu_3\text{-P})_2(\text{CO})_{10}]$  (R = Xyl, <sup>t</sup>Bu), with P–W lengths of ca. 2.29 Å and P→W(CO)<sub>5</sub> lengths of ca. 2.50 Å.<sup>33</sup> However, in the cluster  $[\text{W}_3(\text{C}_5\text{H}_4\text{Bu})_3(\mu_3\text{-P})(\text{CO})_7]$ , the W–P lengths are comparable to those above,<sup>34</sup> even if the long P–W bond now involves a 17-electron  $\text{W}(\text{CO})_3\text{Cp}$  fragment. In order to further clarify the  $\pi(\text{P}-\text{M})$  interactions in our complexes, we carried out density functional theory (DFT) calculations on **4d** and analyzed the corresponding molecular orbitals (see the Supporting Information, SI), as well as the electron density in the M–M and M–P bonds, as managed under the atoms-in-molecules framework.<sup>35</sup>

The DFT-optimized geometry of **4d** (Figure 4) is in good agreement with the structure determined crystallographically,

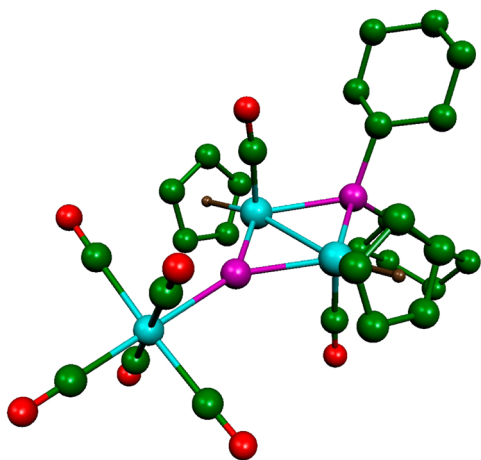


**Figure 4.** DFT-optimized structure of compound **4d**, with H atoms omitted for clarity. Selected bond lengths (Å): Mo–Mo = 2.797; Mo–PCy<sub>2</sub> = 2.456 and 2.448; Mo–P = 2.335 and 2.330; W–P = 2.516.

with computed distances involving the metal atoms a bit longer than the experimental figures, as was usually found in these sorts of calculations. Bonding at the central Mo<sub>2</sub>P<sub>2</sub> core is strongly reminiscent of that computed for the 32-electron carbyne complex  $[\text{Mo}_2\text{Cp}_2(\mu\text{-CCO}_2\text{Me})(\mu\text{-PCy}_2)(\text{CO})_2]$  at the same level of theory.<sup>25c</sup> The Mo–Mo double bond in **4d** follows from a configuration of the type  $\delta^2\sigma^2\pi^2\delta^{*2}$ , with the  $\delta^*$  orbital (HOMO–1, MO166) involved in back-bonding to the carbonyls, while the  $\delta$  orbital (MO159) is strongly stabilized through mixing with the  $p_\pi$  orbital of the phosphide ligand, thus accounting for the  $\pi(\text{P}-\text{Mo})$  interaction within the Mo<sub>2</sub>P ring (Figure 5). We note that the latter orbital also contains some contribution of the W atom, thus pointing to some involvement of the latter in  $\pi$  bonding with the phosphide ligand, but the extent of this interaction is difficult to quantify from a simple orbital analysis. To further clarify this point, we then examined

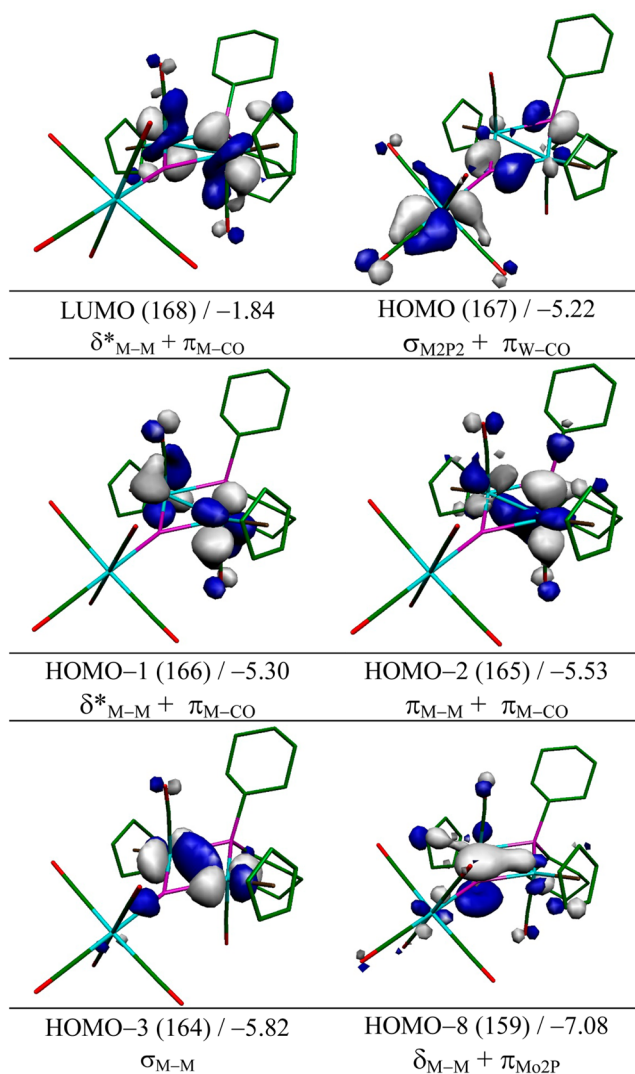


**Figure 5.** Selected molecular orbitals computed for **4d**, with their energies (in eV) and main bonding character indicated below.

the electron densities ( $\rho$ ) at the bond critical points (bcp's) of the bonds of interest (Table 5). First we noticed that the electron density at the Mo–Mo bcp (0.394 e Å<sup>–3</sup>) is only slightly lower than the value computed for the mentioned carbyne complex (0.444 e Å<sup>–3</sup>), substantially higher than the values of ca. 0.2 e Å<sup>–3</sup> computed for single Mo–Mo bonds in related species,<sup>25c</sup> and therefore consistent with the double

**Table 5.** Topological Properties of the Electron Density at the bcp's<sup>a</sup>

bond	4d		4d-W		5 <sup>b</sup>	
	$\rho$	$\nabla^2\rho$	$\rho$	$\nabla^2\rho$	$\rho$	$\nabla^2\rho$
Mo1–Mo2	0.394	0.923	0.419	1.046	not located	
Mo1–P	0.653	2.851	0.668	2.260	0.731	3.371
Mo2–P	0.658	2.836	0.672	2.252	0.370	1.403
W/Mn–P	0.439	3.623			0.628	4.039
Mo1–PCy	0.524	3.018	0.519	3.156	0.551	3.346
Mo2–PCy	0.534	2.976	0.527	3.113	0.398	2.160

<sup>a</sup>Values of the electron density at the bcp's ( $\rho$ ) are given in e Å<sup>–3</sup>, and those of its Laplacian at these points ( $\nabla^2\rho$ ) are given in e Å<sup>–5</sup>. <sup>b</sup>Mo2 refers to the atom bearing two CO ligands.



intermetallic bond formulated for this molecule. As for the bonds involving the phosphide ligand, we note that the electron density at the Mo–P bcp's (ca.  $0.65 \text{ e } \text{\AA}^{-3}$ ) is substantially higher than those at the strong single bonds of the PCy<sub>2</sub> ligand (ca.  $0.53 \text{ e } \text{\AA}^{-3}$ ), somewhat higher than the value of ca.  $0.59 \text{ e } \text{\AA}^{-3}$  computed for the more congested phosphinidene-bridged complex [Mo<sub>2</sub>Cp<sub>2</sub>(μ-PMes\*)(μ-CO)<sub>2</sub>] (with a formal Mo–P bond order of 1.5), and nearly identical with the figure of  $0.654 \text{ e } \text{\AA}^{-3}$  computed for the Mo–P double bond in [Mo<sub>2</sub>Cp<sub>2</sub>(μ-PH)(CO)<sub>2</sub>(η<sup>6</sup>-HMes\*)].<sup>36</sup> All of this is indicative of a strong π interaction between the phosphide ligand and Mo atoms. In contrast, the electron density at the W–P bpc ( $0.439 \text{ e } \text{\AA}^{-3}$ ) is even lower than those involving the PCy<sub>2</sub> ligand and therefore points to a single bond interaction with negligible π contribution from the phosphide ligand. In fact, the electron density computed for a hypothetical WP(CO)<sub>5</sub> molecule with a W–P fixed length of 2.516 Å (the value in the optimized structure of **4d**) is not lower but slightly higher ( $0.492 \text{ e } \text{\AA}^{-3}$ ) surely because of increased back-bonding from the tungsten-based orbitals. Moreover, we note that electron distribution within the Mo<sub>2</sub>P ring is little perturbed upon removal of the full W(CO)<sub>5</sub> fragment to yield a molecule with a bent μ<sub>2</sub>-P ligand [Mo<sub>2</sub>Cp<sub>2</sub>(μ<sub>2</sub>-P)(μ-PCy<sub>2</sub>)(CO)<sub>2</sub>] (**4d-W**; see the SI). Indeed, the electron density at the Mo–P bcp in **4d-W** ( $0.67 \text{ e } \text{\AA}^{-3}$ ; Table 5) is only marginally higher than that in **4b**, with this further indicating that π interaction of the W atom with the phosphide ligand in **4b** is negligible.

In summary, from the precedent analysis, we conclude that π interaction of the phosphide ligand in **4d** is essentially located over the Mo<sub>2</sub>P triangle, much in the same way as π interaction of a bridging carbyne ligand, whereas its interaction with the W atom is best described as just a single donor P→W bond. Thus, we can think of the P→W(CO)<sub>5</sub> fragment as an isolobal analogue of a carbyne ligand (CR). Indeed, the frontier orbitals of such a phosphide fragment (see the SI) are like those of a carbyne,<sup>37,38</sup> and such an analogy will be useful to guide and interpret the reactivity of compounds **4** to be discussed later on.

**Solution Structure of Compounds 3 and 4.** As mentioned earlier, the diphosphenyl complexes **3b** and **3d** could only be partially characterized in solution by IR and <sup>31</sup>P NMR inspection of the crude reaction mixtures because of their low stability (Table 3). Unambiguous assignment of the CO stretches of **3b** could not be done, while the IR spectrum of **3d** was dominated by bands attributed to its W(CO)<sub>5</sub> fragment [2065 (w), 1938 (vs) and 1918 (m, sh) cm<sup>-1</sup>]. Their <sup>31</sup>P{<sup>1</sup>H} NMR spectra display three different resonances in each case, with the most deshielded one (δ<sub>p</sub> ca. 150 ppm) being assigned to the PCy<sub>2</sub> ligand by analogy with the parent methyl-diphosphenyl complex and related compounds.<sup>1</sup> The diphosphenyl ligand gives rise to two upfield doublets in each case, displaying a large J<sub>pp</sub> value above 400 Hz, which is indicative of direct P–P bonding, and individual assignment of these resonances in **3d** to the PMe (δ<sub>p</sub> –154.9 ppm) and P (δ<sub>p</sub> –236.7 ppm) atoms could be unambiguously made by a comparison of the <sup>1</sup>H-decoupled and undecoupled spectra. Assignment of the broad resonances observed for the manganese compound **3b** was made on the assumption that, compared to **3d**, the P resonance should be largely shifted downfield because of the change in metal (Mn vs W), leading to its identification with the –42.9 ppm resonance. Indeed, we have shown previously that resonances of heterometal-bound P atoms in diphosphorus-bridged complexes [Mo<sub>2</sub>MCp<sub>2</sub>(μ-κ<sup>2</sup>:κ<sup>2</sup>:κ<sup>1</sup>-P<sub>2</sub>)(μ-PCy<sub>2</sub>)(CO)<sub>2</sub>L<sub>n</sub>] move upfield by some 100 ppm as we go from

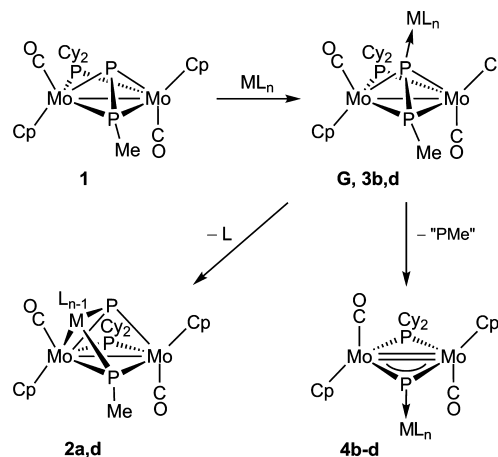
first- to second-row metals and by a similar amount as we go from second- to third-row metals.<sup>1b</sup>

Spectroscopic data in solution for compounds **4** are consistent with the solid-state structure of **4d**. Once more, bands due to the Mo<sub>2</sub>(CO)<sub>2</sub> oscillator were not appreciated in the solution IR spectra for these complexes, which instead were dominated by the bands arising from the ML<sub>n</sub> fragments terminally bound to the phosphide ligand (MnCp'(CO)<sub>2</sub> and M(CO)<sub>5</sub>). Yet, the <sup>1</sup>H and <sup>13</sup>C{<sup>1</sup>H} NMR spectra of these compounds are as expected for molecules with a C<sub>2</sub> axis containing both P nuclei, thus rendering CO, Cp, and Cy pairs equivalent in the Mo<sub>2</sub> unit. The most remarkable spectroscopic feature of compounds **4**, however, is found in their <sup>31</sup>P{<sup>1</sup>H} NMR spectra, which in each case display two negligibly coupled resonances, as were typically found for mixed PR<sub>2</sub> complexes of the type *trans*-[M<sub>2</sub>Cp<sub>2</sub>(μ-PR<sub>2</sub>)(μ-PR'<sub>2</sub>)(CO)<sub>2</sub>] also having planar M<sub>2</sub>P<sub>2</sub> cores.<sup>39</sup> The PCy<sub>2</sub> group in compounds **4** give rise to a resonance at ca. 120 ppm, a position comparable to those found in the mentioned mixed complexes. In contrast, the phosphide ligand gives rise to a dramatically deshielded resonance at around 1100 ppm, which is characteristic of trigonal-planar phosphide ligands coordinated to three metal centers. Yet, this shift still is substantially higher than those measured for related phosphide-bridged complexes involving similar metal atoms (cf. 885 ppm for [W<sub>2</sub>Re<sub>2</sub>Cp\*<sub>2</sub>(μ<sub>3</sub>-P)<sub>2</sub>(CO)<sub>12</sub>],<sup>7</sup> 882.5 ppm for [MoW<sub>2</sub>Cp(μ<sub>3</sub>-P)(CO)<sub>12</sub>],<sup>14</sup> or even 558.2 ppm for [W<sub>4</sub>(OXyl)<sub>4</sub>(μ<sub>3</sub>-P)<sub>2</sub>(CO)<sub>10</sub>].<sup>33a</sup>

#### Reaction Pathways to the Trinuclear Derivatives of 1.

In spite of the diverse output of the reactions of **1** with different metal carbonyl solvates discussed so far, these all seem to be initiated analogously, then evolving differently depending on the nature of each particular metal fragment being added (Scheme 3). The first step in all cases would be the

Scheme 3



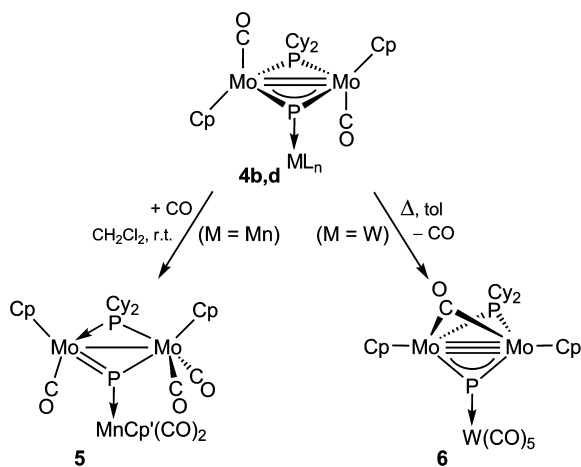
incorporation of a 16-electron metal fragment ML<sub>n</sub> [Fe(CO)<sub>4</sub>, W(CO)<sub>4</sub>(THF), MnCp'(CO)<sub>2</sub>, Mo(CO)<sub>5</sub>, W(CO)<sub>5</sub>] to the P atom bearing the LP in the diphosphenyl ligand, to yield κ<sup>2</sup>:κ<sup>2</sup>:κ<sup>1</sup>-diphosphenyl intermediates of type F only detected in some cases (**3b** and **3d**). When the added fragment is W(CO)<sub>4</sub>(THF), this first step would be naturally followed by THF dissociation and insertion of the resulting unsaturated W(CO)<sub>4</sub> fragment in the P–P bond of the diphosphenyl ligand and creation of a new W–Mo bond, to eventually give the phosphide phosphinidene complex **2d**. Formation of the iron product **2a** likely would proceed analogously from the

corresponding intermediate of type G, after spontaneous decarbonylation of the  $\text{Fe}(\text{CO})_4$  fragment. Interestingly, the first step in the suggested sequence leading to compounds **2** is related to the electrophilic activation of  $\text{P}_4$  by silylenes, phosphonium cations, and related carbene-like species,<sup>40</sup> a process also resulting in the eventual insertion of the added electrophile in a P–P bond. In contrast, intermediates of type G not releasing easily a ligand from the  $\text{ML}_n$  fragment [as is the case of fragments  $\text{MnCp}'(\text{CO})_2$  and  $\text{W}(\text{CO})_5$ ] would alternatively evolve through extrusion of the phosphinidene “PMe” moiety to give compounds **4**. It is difficult to identify the origin of the low stability of type G intermediates in these reactions, but the steric pressure introduced by the relatively bulky  $\text{ML}_n$  fragments being added might be a major factor contributing to this effect. The case of the  $\text{Mo}(\text{CO})_5$  fragment stands apart because three different intermediates, none of them with a structure of type G, seem to precede formation of the corresponding phosphide derivative **4c**, as noted above, and we will not speculate about their possible nature.

**Carbon Monoxide (CO) Uptake and Release in Phosphide-Bridged Complexes 4.** We have shown above that, at the structural and electronic levels, the phosphide-bridged complexes **4** can be related to carbyne complexes of the type  $[\text{Mo}_2\text{Cp}_2(\mu\text{-CX})(\mu\text{-PCy}_2)(\text{CO})_2]$  by virtue of the isolobal relationship between the  $\text{PW}(\text{CO})_5$  and CX moieties, and we might ask whether this analogy can also be extended to their chemical behavior. As a proof of concept to address this question, we have examined carbonylation and decarbonylation reactions of some of these phosphide complexes.

The 32-electron carbyne complexes mentioned above have been shown to be carbonylated to give either ketenyl  $[\text{Mo}_2\text{Cp}_2\{\mu\text{-C}(\text{X})\text{CO}\}(\mu\text{-PCy}_2)(\text{CO})_2]$  or tricarbonyl  $[\text{Mo}_2\text{Cp}_2(\mu\text{-CX})(\mu\text{-PCy}_2)(\text{CO})_3]$  derivatives, depending on X (OMe, Ph).<sup>25c,b</sup> The manganese complex **4b** readily reacts with CO under mild conditions (293 K, 3 bar) to give the pentacarbonyl derivative  $[\text{MnMo}_2\text{Cp}_2\text{Cp}'(\mu_3\text{-P})(\mu\text{-PCy}_2)(\text{CO})_5]$  (**5**), an electron-precise molecule following from coordination of a CO molecule and trans-to-cis rearrangement of the  $\text{Mo}_2\text{Cp}_2$  moiety (Scheme 4). This reaction thus matches exactly the carbonylation of the methoxycarbyne complex  $[\text{Mo}_2\text{Cp}_2(\mu\text{-COMe})(\mu\text{-PCy}_2)(\text{CO})_2]$ , including the trans-to-cis rearrangement, a behavior also shown by some other isoelectronic species such as the alkenyl complexes  $[\text{Mo}_2\text{Cp}_2(\mu\text{-}\eta^1\text{:}\eta^2\text{-CHCHR})(\mu\text{-PCy}_2)(\text{CO})_2]$  (R = H, p-

Scheme 4



toly) and even by the diethylphosphide complex  $[\text{Mo}_2\text{Cp}_2(\mu\text{-PEt}_2)(\text{CO})_2]$ .<sup>39</sup> We note that compound **5** is a rather unstable molecule that starts to release CO upon removal of the CO atmosphere, to regenerate the parent compound **4b**. Yet, we were able to grow a few crystals of it, thus enabling its full structural characterization, to be discussed below.

On the other hand, we have shown previously that the carbyne complexes  $[\text{Mo}_2\text{Cp}_2(\mu\text{-CX})(\mu\text{-PCy}_2)(\text{CO})_2]$  usually require photochemical activation in order to remove a CO molecule from them, although the benzyldiene complex (X = Ph) can be decarbonylated very slowly in refluxing toluene solutions.<sup>25b,c</sup> In all cases, however, the product formed is the corresponding 30-electron monocarbonyl  $[\text{Mo}_2\text{Cp}_2(\mu\text{-CX})(\mu\text{-PCy}_2)(\mu\text{-CO})]$  with a Mo–Mo triple bond.<sup>42</sup> In a similar way, the tungsten complex **4d** was decarbonylated in a refluxing toluene solution to give  $[\text{Mo}_2\text{WCp}_2(\mu_3\text{-P})(\mu\text{-PCy}_2)(\mu\text{-CO})(\text{CO})_5]$  (**6**), a molecule retaining an intact  $\text{PW}(\text{CO})_5$  fragment bound to an unsaturated dimolybdenum center now formally bearing an intermetallic triple bond (Scheme 4).

**Solid-State and Solution Structure of 5.** The molecule of **5** in the crystal is built from  $\text{MoCp}(\text{CO})$  and  $\text{MoCp}(\text{CO})_2$  fragments directly bonded to each other and displaying a cisoid arrangement of the Cp ligands (Figure 6 and Table 6). These

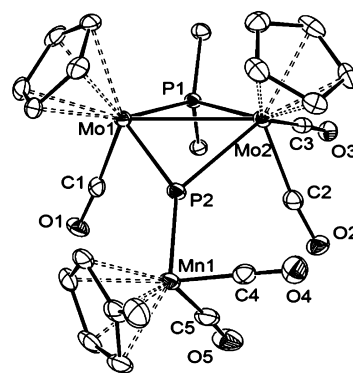


Figure 6. ORTEP diagram (30% probability) of compound **5** with H atoms and Cy groups (except the C1 atoms) omitted for clarity.

Table 6. Selected Bond Lengths (Å) and Angles (deg) for Compound **5**

Mo1–Mo2	3.1318(7)	P2–Mo1–P1	94.95(5)
Mo1–P1	2.385(1)	P2–Mo2–P1	83.22(5)
Mo2–P1	2.551(2)	Mo1–P1–Mo2	78.69(5)
Mo1–P2	2.233(2)	Mo1–P2–Mo2	80.91(5)
Mo2–P2	2.577(1)	Mo1–P2–Mn1	143.21(8)
P2–Mn1	2.153(2)	Mo2–P2–Mn1	135.82(8)
Mo1–C1	1.942(6)	C1–Mo1–Mo2	111.5(2)
Mo2–C2	1.933(6)	C2–Mo2–Mo1	111.3(2)
Mo2–C3	1.961(6)	C3–Mo2–Mo1	116.6(2)
Mn1–C4	1.784(7)	C2–Mo2–C3	76.5(2)
Mn1–C5	1.787(7)	C4–Mn1–C5	91.5(3)

two fragments are bridged by a  $\text{PCy}_2$  ligand and by a trigonal planar phosphide ligand (P2), which is also coordinated to an exocyclic  $\text{MnCp}'(\text{CO})_2$  fragment. The corresponding Mn–P distance of 2.153(2) Å is comparable to the value measured for the phosphite complex  $[\text{Mn}(\eta^5\text{-triindane})(\text{CO})_2\{\text{P}(\text{OMe})_3\}]$  (2.1673(6) Å)<sup>43</sup> and is therefore consistent with the formulation of a single dative bond for this interaction, as



found for **4d**. The Mo–Mo distance of 3.1318(7) Å is consistent with a single Mo–Mo bond, as predicted under the 18-electron formalism while using the isolobal relationship discussed above, which implies a 3-electron contribution of the P→MnCp'(CO)<sub>2</sub> fragment to the dimetal unit, and is only marginally longer than those measured for related species such as the alkenyl complex [Mo<sub>2</sub>Cp<sub>2</sub>(μ-η<sup>1</sup>:η<sup>2</sup>-CHCH<sub>2</sub>)(μ-PCy<sub>2</sub>)(CO)<sub>3</sub>] [3.0858(7) Å]<sup>41a</sup> but ca. 0.34 Å longer than the figure of 2.749(2) Å measured for the Mo–Mo double bond in **4d**. The P atoms bridging the Mo<sub>2</sub> unit define a puckered PMo<sub>2</sub>P rhombus (P1–Mo2–Mo1–P2 = ca. 132°) with distances to Mo1 substantially shorter than those to Mo2, thus balancing the lower coordination number of the former atom. The Mo1–PCy<sub>2</sub> length of 2.385(1) Å is ca. 0.15 Å shorter than the Mo2–PCy<sub>2</sub> one [2.551(2) Å], therefore consistent with formal P→Mo1 and P–Mo2 descriptions for these bonds. As for the phosphide ligand, the Mo1–P and Mo2–P lengths [2.233(2) and 2.577(1) Å] are respectively shorter and much longer than the average value of ca. 2.30 Å measured for the symmetrical phosphide ligand in **4d**, thus supporting the formulation of Mo–P double and single bonds, respectively (Scheme 3).<sup>36</sup> The phosphide asymmetry in **5** is thus more pronounced than those found for the complexes [Cr<sub>2</sub>WCp(μ<sub>3</sub>-P)(CO)<sub>12</sub>]<sub>44</sub> and [MoW<sub>2</sub>(μ<sub>3</sub>-P)Cp(CO)<sub>12</sub>]<sub>14</sub> which display short M–P lengths of ca. 2.26 and 2.30 Å, respectively.

To further support our description of the phosphide bonding in **5**, we carried out DFT calculations analogous to those discussed for **4d** (see the SI). The optimized structure is comparable to the one determined crystallographically, with the phosphide ligand bridging the Mo atoms very asymmetrically (Mo–P = 2.251 and 2.678 Å). The molecular orbitals in this case are heavily mixed and therefore little informative in this respect, but the electron density at the Mo1–P bcp (0.731 e Å<sup>-3</sup>; Table 5) is substantially higher than the value of ca. 0.65 e Å<sup>-3</sup> for the symmetrical phosphide in **4d** and nearly doubles the figure for the long Mo2–P bond (0.370 e Å<sup>-3</sup>), all of this being consistent with the formulations of Mo–P double and single bonds, respectively.

Spectroscopic data in solution for **5** are in good agreement with its solid-state structure. Its IR spectrum displays four rather than the five C–O stretches expected from the superimposition of bands arising from independent Mo<sub>2</sub>(CO)<sub>3</sub> and Mn(CO)<sub>2</sub> oscillators, surely as a result of the accidental degeneracy of two of them. Its <sup>31</sup>P{<sup>1</sup>H} NMR spectrum displays the characteristic strongly deshielded resonance corresponding to the trigonal-planar phosphide (δ<sub>p</sub> 951.0 ppm), which now is visibly coupled (<sup>2</sup>J<sub>PP</sub> = 11 Hz) to the PCy<sub>2</sub> resonance (δ<sub>p</sub> 223.2 ppm), thus reflecting the reduced P–Mo–P angle in this molecule (average 89°) compared to **4d** (ca. 109°).<sup>45</sup> We note that the PCy<sub>2</sub> resonance in **5** is 100 ppm higher than that in the precursor **4b**. This is a general trend found when related couples of complexes are compared with formal Mo–Mo double and single bonds, such as [Mo<sub>2</sub>Cp<sub>2</sub>(μ-PEt<sub>2</sub>)<sub>2</sub>(CO)<sub>n</sub>] (δ<sub>p</sub> 78.7 and 194.7 ppm for *n* = 2 and 3),<sup>39</sup> [Mo<sub>2</sub>Cp<sub>2</sub>(μ-η<sup>1</sup>:η<sup>2</sup>-CHCH<sub>2</sub>)(μ-PCy<sub>2</sub>)(CO)<sub>n</sub>] (δ<sub>p</sub> 135.0 and 250.5 ppm for *n* = 2 and 3),<sup>41</sup> or [Mo<sub>2</sub>Cp<sub>2</sub>(μ-COMe)(μ-PCy<sub>2</sub>)(CO)<sub>n</sub>] (δ<sub>p</sub> 125.0 and 219.7 ppm for *n* = 2 and 3).<sup>25c</sup>

**Solution Structure of 6.** Although crystals suitable for X-ray analysis could not be obtained for this compound, spectroscopic data in solution are enough to define its structure (Scheme 4). Its IR spectrum exhibits two bands at high frequencies [2063 (m) and 1941 (vs) cm<sup>-1</sup>] corresponding to the W(CO)<sub>5</sub> fragment and a weaker band at low frequency

(1714 cm<sup>-1</sup>) characteristic of a bridging CO ligand, also identified through its strongly deshielded <sup>13</sup>C NMR resonance (δ<sub>c</sub> 296.8 ppm). The <sup>31</sup>P{<sup>1</sup>H} NMR spectrum of **6** displays the expected highly deshielded resonance corresponding to the μ<sub>3</sub>-P ligand (δ<sub>p</sub> 925.2 ppm), which is also appreciably coupled (<sup>2</sup>J<sub>PP</sub> = 30 Hz) to the PCy<sub>2</sub> resonance (δ<sub>p</sub> 246.0 ppm). Indeed, <sup>2</sup>J<sub>PP</sub> couplings in the related triply bonded monocarbonyls [Mo<sub>2</sub>Cp<sub>2</sub>(μ-PR<sub>2</sub>)(μ-PR'R')(μ-CO)] fall in the range 20–30 Hz, and their <sup>31</sup>P chemical shifts also are very high (cf. 263.7 ppm for [Mo<sub>2</sub>Cp<sub>2</sub>(μ-PCy<sub>2</sub>)<sub>2</sub>(μ-CO)]).<sup>39</sup> The <sup>1</sup>H and <sup>13</sup>C{<sup>1</sup>H} NMR spectra are indicative of a structure having a symmetry plane containing the P atoms bridging the Mo<sub>2</sub> unit, thus rendering the Cp ligands equivalent. Yet, the Cy groups remain inequivalent, as indicated by the presence of eight resonances (four per group) in the <sup>13</sup>C{<sup>1</sup>H} NMR spectrum. Again, fast rotation on the NMR time scale around the P–W bond renders the equatorial CO ligands of the W(CO)<sub>5</sub> fragment equivalent, as denoted by the presence of a single resonance corresponding to these four ligands (197.5 ppm) and a separated one for the axial carbonyl (206.4 ppm), in a 4:1 intensity ratio.

## CONCLUSIONS

The methyldiphosphenyl complex **1** easily incorporates 16-electron ML<sub>n</sub> fragments to give unstable trinuclear diphosphenyl complexes [Mo<sub>2</sub>MCp<sub>2</sub>(μ-PCy<sub>2</sub>)(μ<sub>3</sub>-κ<sup>2</sup>:κ<sup>2</sup>:κ<sup>1</sup>-P<sub>2</sub>Me)(CO)<sub>2</sub>L<sub>n</sub>] evolving via two main pathways: (a) release of an L ligand (L = THF, CO) with concomitant P–P bond cleavage and formation of a new Mo–M bond to give phosphide- and phosphinidene-bridged derivatives of the type [Mo<sub>2</sub>MCp<sub>2</sub>(μ<sub>3</sub>-P)(μ-PCy<sub>2</sub>)(μ<sub>3</sub>-PMe)L<sub>n-1</sub>]; (b) release of PMe to give the corresponding phosphide-bridged derivatives [Mo<sub>2</sub>MCp<sub>2</sub>(μ<sub>3</sub>-P)(μ-PCy<sub>2</sub>)(CO)<sub>2</sub>L<sub>n</sub>]. The latter display trigonal-planar phosphide ligands involved in strong π bonding with the unsaturated Mo<sub>2</sub> center of these molecules, while M–P interaction with the exocyclic ML<sub>n</sub> fragment can be described as a single dative bond, a view further supported by DFT calculations, which also allows us to identify an isolobal analogy between the P→ML<sub>n</sub> fragments in these products and a carbyne ligand (CR). The latter analogy enables, in turn, an easy interpretation and prediction of the reactivity of these unsaturated complexes concerning their uptake and release of simple ligands such as CO, which reproduces the chemical behavior of carbyne-bridged complexes [Mo<sub>2</sub>Cp<sub>2</sub>(μ-CX)(μ-PCy<sub>2</sub>)(CO)<sub>2</sub>] and related molecules.

## EXPERIMENTAL SECTION

**General Procedures and Starting Materials.** All manipulations and reactions were carried out under a N<sub>2</sub> (99.995%) atmosphere using standard Schlenk techniques. Solvents were purified according to literature procedures and distilled prior to use.<sup>46</sup> All reagents were obtained from the usual commercial suppliers and used as received, unless otherwise stated, except for compounds [MnCp'(CO)<sub>2</sub>(THF)],<sup>47</sup> [M(CO)<sub>5</sub>(THF)] (M = Mo, W),<sup>48</sup> and [Mo<sub>2</sub>Cp<sub>2</sub>(μ-PCy<sub>2</sub>)(μ-κ<sup>2</sup>:κ<sup>2</sup>-P<sub>2</sub>Me)(CO)<sub>2</sub>] (**1**),<sup>1</sup> which were prepared as described previously. Photochemical experiments were performed using jacketed Pyrex Schlenk tubes, cooled by tap water (ca. 288 K). A 400 W mercury lamp placed ca. 1 cm away from the Schlenk tube was used for these experiments. Modified literature procedures were employed in the preparation of adducts [M(CO)<sub>4</sub>(THF)<sub>2</sub>] (M = Mo, W);<sup>49</sup> the molybdenum complex was obtained at 288 K at low reaction times, whereas formation of the tungsten complex required longer reaction times (1.5–2 h) and lower temperatures (273 K). In both cases, IR monitoring was used to determine the optimum reaction time. Petroleum ether refers to that fraction distilling in the range

338–343 K. Chromatographic separations were carried out using jacketed columns refrigerated by tap water or by a closed 2-propanol circuit kept at the desired temperature with a cryostat. Commercial aluminum oxide (activity I, 150 mesh) was degassed under vacuum prior to use. The latter was mixed under N<sub>2</sub> with the appropriate amount of water to reach activity IV. IR stretching frequencies of CO ligands measured in solution (using CaF<sub>2</sub> windows), or in Nujol mulls, are referred to as  $\nu(\text{CO})$  and are given in wave numbers (cm<sup>-1</sup>). NMR spectra were routinely recorded at 300.13 (<sup>1</sup>H), 121.50 (<sup>31</sup>P{<sup>1</sup>H}), or 75.47 (<sup>13</sup>C{<sup>1</sup>H}) MHz at 298 K in a CD<sub>2</sub>Cl<sub>2</sub> solution unless otherwise stated. Chemical shifts ( $\delta$ ) are given in ppm, relative to internal tetramethylsilane (<sup>1</sup>H and <sup>13</sup>C) or external 85% aqueous H<sub>3</sub>PO<sub>4</sub> solutions (<sup>31</sup>P). Coupling constants (*J*) are given in hertz.

**Preparation of [Mo<sub>2</sub>FeCp<sub>2</sub>( $\mu$ -P)( $\mu$ -PCy<sub>2</sub>)( $\mu$ <sub>3</sub>-PMe)(CO)<sub>5</sub>] (2a).** Solid [Fe<sub>2</sub>(CO)<sub>9</sub>] (0.025 g, 0.070 mmol) was added to a solution of compound **1** (0.045 g, 0.069 mmol) in dichloromethane (5 mL), and the mixture was stirred for 1 h at room temperature to give a brown-orange solution mainly containing compound **2a**, along with smaller amounts of a tetranuclear derivative. Solvent was then removed under vacuum, the residue was extracted with dichloromethane/petroleum ether (1:9), and the extracts were chromatographed through alumina at 288 K. An orange fraction was eluted with the same solvent mixture, which gave, after removal of solvents, compound **2a** as an orange microcrystalline solid (0.020 g, 36%). Crystals suitable for X-ray analysis were grown by slow diffusion of a layer of petroleum ether into a concentrated toluene solution of the complex at 253 K. Anal. Calcd for C<sub>28</sub>H<sub>35</sub>FeMo<sub>2</sub>O<sub>3</sub>P<sub>3</sub>: C, 42.45; H, 4.45. Found: C, 42.58; H, 4.64. IR [ $\nu(\text{CO})$ , Nujol]: 2010 (s), 1950 (s), 1936 (s), 1903 (vs), 1868 (m), 1829 (w, sh). <sup>1</sup>H NMR:  $\delta$  5.34 (d, *J*<sub>PH</sub> = 1, 5H, Cp), 5.22 (s, 5H, Cp), 2.37 (d, *J*<sub>PH</sub> = 8, 3H, PMe), 1.90–1.10 (m, 22H, Cy). <sup>31</sup>P{<sup>1</sup>H} NMR:  $\delta$  268.2 (d, *J*<sub>PP</sub> = 14,  $\mu$ <sub>3</sub>-PMe), 239.2 (d, *J*<sub>PP</sub> = 9,  $\mu$ <sub>3</sub>-P), 151.4 (dd, *J*<sub>PP</sub> = 14, 9,  $\mu$ -PCy<sub>2</sub>). <sup>31</sup>P NMR:  $\delta$  268.2 (m, br,  $\mu$ <sub>3</sub>-PMe), 239.2 (d, br, *J*<sub>PP</sub> = 9,  $\mu$ <sub>3</sub>-P), 151.4 (m,  $\mu$ -PCy<sub>2</sub>). <sup>13</sup>C{<sup>1</sup>H} NMR:  $\delta$  236.9 (s, br, MoCO), 229.1 (d, *J*<sub>CP</sub> = 40, MoCO), 212.8 (s, 3FeCO), 88.0, 87.9 (2s, Cp), 52.2 [dd, *J*<sub>CP</sub> = 9, 2, C1(Cy)], 43.8 [dd, *J*<sub>CP</sub> = 11, 11, C1(Cy)], 37.5 [s, C2(Cy)], 36.1 [s, 2C2(Cy)], 34.3 [d, *J*<sub>CP</sub> = 5, C2(Cy)], 29.6 (d, *J*<sub>CP</sub> = 47, PMe), 28.9 [d, *J*<sub>CP</sub> = 11, C3(Cy)], 28.3 [d, *J*<sub>CP</sub> = 10, 2C3(Cy)], 28.2 [d, *J*<sub>CP</sub> = 8, C3(Cy)], 26.4, 26.2 [2s, C4(Cy)].

**Preparation of [Mo<sub>2</sub>WCp<sub>2</sub>( $\mu$ -P)( $\mu$ -PCy<sub>2</sub>)( $\mu$ <sub>3</sub>-PMe)(CO)<sub>6</sub>] (2d).** A THF solution (5 mL) of the adduct [W(CO)<sub>4</sub>(THF)<sub>2</sub>], prepared in situ from [W(CO)<sub>6</sub>] (0.017 g, 0.048 mmol), was added to a THF solution (5 mL) of compound **1** (0.030 g, 0.046 mmol), and the mixture was stirred for 50 min to give a brown-orange solution containing compounds **2d** and **3d** in a ratio of ca. 5:2, along with small amounts of **4d**. Solvent was then removed under vacuum, the residue was extracted with dichloromethane/petroleum ether (1:8), and the extracts were chromatographed through alumina at 288 K. Elution with dichloromethane/petroleum ether (1:5) gave a brown-gray fraction, yielding, after removal of solvents, compound **2d** as a brown solid (0.027 g, 62%). The crystals used in the X-ray study were grown by the slow diffusion of a layer of petroleum ether into a concentrated dichloromethane solution of the complex at 253 K. Anal. Calcd for C<sub>29</sub>H<sub>35</sub>Mo<sub>2</sub>O<sub>6</sub>P<sub>3</sub>W: C, 36.73; H, 3.72. Found: C, 37.46; H, 3.69. <sup>1</sup>H NMR:  $\delta$  5.39 (s, br, 5H, Cp), 5.24 (d, *J*<sub>PH</sub> = 1, 5H, Cp), 2.21 (m, 1H, Cy), 1.95 (d, *J*<sub>PH</sub> = 5, 3H, PMe), 1.90–1.10 (m, 21H, Cy). <sup>31</sup>P{<sup>1</sup>H} NMR:  $\delta$  321.5 (s, br,  $\mu$ <sub>3</sub>-PMe), 165.7 (s, br,  $\mu$ -PCy<sub>2</sub>), 124.5 (s, br,  $\mu$ <sub>3</sub>-P). <sup>13</sup>C{<sup>1</sup>H} NMR:  $\delta$  215.9 (s, WCO), 91.1, 88.6 (2s, Cp), 51.4 [dd, *J*<sub>CP</sub> = 7, 5, C1(Cy)], 37.8 [s, C2(Cy)], 36.7 [s, 2C2(Cy)], 36.4 [dd, *J*<sub>CP</sub> = 6, 4, C1(Cy)], 34.0 [d, *J*<sub>CP</sub> = 5, C2(Cy)], 29.2 [d, *J*<sub>CP</sub> = 11, C3(Cy)], 29.2 [d, *J*<sub>CP</sub> = 43, PMe], 28.7, 28.6 [2d, *J*<sub>CP</sub> = 11, C3(Cy)], 28.3 [d, *J*<sub>CP</sub> = 8, C3(Cy)], 26.6 [s, br, 2C4(Cy)]; the resonances corresponding to the molybdenum-bound CO ligands could not be clearly identified in this spectrum.

**Preparation of Solutions of [MnMo<sub>2</sub>Cp<sub>2</sub>Cp'( $\mu$ -PCy<sub>2</sub>)( $\mu$ <sub>3</sub>- $\kappa^2$ - $\kappa^1$ -P<sub>2</sub>Me)(CO)<sub>4</sub>] (3b).** A THF solution (5 mL) of the adduct [MnCp'(CO)<sub>2</sub>(THF)], prepared in situ from [MnCp'(CO)<sub>3</sub>] (6  $\mu$ L, 0.038 mmol), was added to a THF solution (5 mL) of compound **1** (0.020 g, 0.031 mmol), and the mixture was stirred at room temperature for 40 min to give a brown-orange solution containing

compound **3b** as the major product, along with small amounts of a tetranuclear compound. These species are both very unstable and decompose upon manipulation to give compound **4b** as the only carbonyl-containing product. <sup>31</sup>P{<sup>1</sup>H} NMR (THF, 162.14 MHz):  $\delta$  157.4 (s, br,  $\mu$ -PCy<sub>2</sub>), -42.9 (d, br, *J*<sub>PP</sub> = 400, PMn), -180.3 (d, br, *J*<sub>PP</sub> = 400, PMe).

**Preparation of Solutions of [Mo<sub>2</sub>WCp<sub>2</sub>( $\mu$ -PCy<sub>2</sub>)( $\mu$ <sub>3</sub>- $\kappa^2$ - $\kappa^1$ -P<sub>2</sub>Me)(CO)<sub>7</sub>] (3d).** A THF solution (5 mL) of the adduct [W(CO)<sub>5</sub>(THF)], prepared in situ from [W(CO)<sub>6</sub>] (0.011 g, 0.031 mmol), was added to a THF solution (5 mL) of compound **1** (0.020 g, 0.031 mmol), and the mixture was stirred for 1 h in a Schlenk tube equipped with a Young's valve to give a brown-orange solution containing compound **3d** as the major species. Attempts to further purify this compound were unsuccessful because of its progressive decomposition to give the phosphide complex **4d**. <sup>31</sup>P{<sup>1</sup>H} NMR (toluene, 162.14 MHz):  $\delta$  148.7 (dd, *J*<sub>PP</sub> = 56, 16,  $\mu$ -PCy<sub>2</sub>), -154.9 (dd, *J*<sub>PP</sub> = 419, 16, PMe), -236.7 (dd, *J*<sub>PP</sub> = 419, 56, PW). <sup>31</sup>P NMR (toluene, 162.14 MHz):  $\delta$  148.7 (d, br, *J*<sub>PP</sub> = 56,  $\mu$ -PCy<sub>2</sub>), -154.9 (d, br, *J*<sub>PP</sub> = 419, PMe), -236.7 (dd, *J*<sub>PP</sub> = 419, 56, PW).

**Preparation of [MnMo<sub>2</sub>Cp<sub>2</sub>Cp'( $\mu$ -P)( $\mu$ -PCy<sub>2</sub>)(CO)<sub>4</sub>] (4b).** A THF solution (5 mL) of compound **1** (0.030 g, 0.046 mmol) was added to a THF solution of the adduct [MnCp'(CO)<sub>2</sub>(THF)], prepared in situ from [MnCp'(CO)<sub>3</sub>] (28  $\mu$ L, 0.178 mmol), and the mixture was stirred at room temperature for 90 min to give a brown-orange solution containing a mixture of **4b** and **3b** in a ratio of ca. 1:1, along with small amounts of a tetranuclear complex. Solvent was then removed, the residue was extracted with dichloromethane/petroleum ether (1:6), and the extracts were chromatographed through alumina at 253 K. Elution with dichloromethane/petroleum ether (1:8) gave first an orange fraction, which was discarded, and then a yellow one, yielding, after removal of solvents, compound **4b** as an orange solid (0.026 g, 71%). Anal. Calcd for C<sub>32</sub>H<sub>39</sub>MnMo<sub>2</sub>O<sub>4</sub>P<sub>2</sub>: C, 48.26; H, 4.94. Found: C, 48.03; H, 4.98. <sup>1</sup>H NMR:  $\delta$  5.76 (s, 10H, Cp), 5.15 (m, 2H, C<sub>2</sub>H<sub>4</sub>), 4.96, 4.94 (2m, 2  $\times$  1H, C<sub>2</sub>H<sub>4</sub>), 2.45 (m, 2H, Cy), 2.02 (s, 3H, Me), 2.0–1.0 (m, 20H, Cy). <sup>31</sup>P{<sup>1</sup>H} NMR:  $\delta$  1103.3 (s,  $\mu$ <sub>3</sub>-P), 117.6 (s,  $\mu$ -PCy<sub>2</sub>). <sup>31</sup>P{<sup>1</sup>H} NMR (161.98 MHz, 223 K):  $\delta$  1094.4 (s,  $\mu$ <sub>3</sub>-P), 116.3 (s,  $\mu$ -PCy<sub>2</sub>). <sup>13</sup>C{<sup>1</sup>H} NMR (100.61 MHz, 223 K):  $\delta$  231.9 (s, br, MoCO), 222.9 (s, br, MnCO), 90.6 (s, Cp), 102.6 [s, C1(C<sub>2</sub>H<sub>4</sub>)], 86.4, 85.5, 85.1, 83.7 [4s, CH(C<sub>2</sub>H<sub>4</sub>)], 43.7 [d, *J*<sub>CP</sub> = 20, C1(Cy)], 35.5 [s, C2(Cy)], 30.3 [s, C2(Cy)], 28.1 [d, *J*<sub>CP</sub> = 12, C3(Cy)], 28.0 [s, *J*<sub>CP</sub> = 12, C3(Cy)], 26.3 [s, br, C4(Cy)], 14.2 (s, Me).

**Preparation of [Mo<sub>3</sub>Cp<sub>2</sub>( $\mu$ -P)( $\mu$ -PCy<sub>2</sub>)(CO)<sub>7</sub>] (4c).** A THF solution (5 mL) of the adduct [Mo(CO)<sub>5</sub>(THF)], prepared in situ from [Mo(CO)<sub>6</sub>] (0.010 g, 0.038 mmol), was added to a THF solution (5 mL) of compound **1** (0.020 g, 0.031 mmol), and the mixture was stirred for 1 h to give a brown solution containing three unidentified products (compounds A–C) in similar amounts. Solvent was then removed under vacuum, the residue was extracted with dichloromethane/petroleum ether (1:3), and the extract was chromatographed through alumina at 253 K. Elution with the same solvent mixture gave a yellow fraction, yielding, after removal of solvents, compound **4c** as a yellow solid (0.020 g, 76%). Anal. Calcd for C<sub>29</sub>H<sub>32</sub>Mo<sub>3</sub>O<sub>7</sub>P<sub>2</sub> (4c): C, 41.35; H, 3.83. Found: C, 41.70; H, 3.81. **Spectroscopic Data for Compound 4c.** <sup>1</sup>H NMR:  $\delta$  5.86 (s, 10H, Cp), 2.50 (m, 2H, Cy), 2.10–1.00 (m, 20H, Cy). **Spectroscopic Data for Compound A.** <sup>31</sup>P{<sup>1</sup>H} NMR (THF):  $\delta$  299.6 (dd, *J*<sub>PP</sub> = 93, 17,  $\mu$ -P), 138.6 (dd, *J*<sub>PP</sub> = 16, 8,  $\mu$ -PCy<sub>2</sub>), 137.9 (dd, *J*<sub>PP</sub> = 93, 8,  $\mu$ -P). **Spectroscopic Data for Compound B.** <sup>31</sup>P{<sup>1</sup>H} NMR (THF):  $\delta$  144.6 (dd, *J*<sub>PP</sub> = 83, 51,  $\mu$ -PCy<sub>2</sub>), 115.8 (dd, *J*<sub>PP</sub> = 146, 83,  $\mu$ -P), 27.2 (dd, *J*<sub>PP</sub> = 146, 51,  $\mu$ -P). **Spectroscopic Data for Compound C.** <sup>31</sup>P{<sup>1</sup>H} NMR (THF):  $\delta$  262.9 (dd, *J*<sub>PP</sub> = 85, 13,  $\mu$ -P), 155.9 (dd, *J*<sub>PP</sub> = 13, 6,  $\mu$ -PCy<sub>2</sub>), 153.0 (dd, *J*<sub>PP</sub> = 85, 6,  $\mu$ -P).

**Preparation of [Mo<sub>2</sub>WCp<sub>2</sub>( $\mu$ -P)( $\mu$ -PCy<sub>2</sub>)(CO)<sub>7</sub>] (4d).** A THF solution (5 mL) of the adduct [W(CO)<sub>5</sub>(THF)], prepared in situ from [W(CO)<sub>6</sub>] (0.011 g, 0.031 mmol), was added to a THF solution (5 mL) of compound **1** (0.020 g, 0.031 mmol), and the mixture was stirred for 50 min. The solvent was then removed under vacuum, the residue dissolved in toluene (7 mL), and the solution stirred for 2 h at 343 K to give an orange solution containing **4d** as the major species. Solvent was then removed under vacuum, the residue extracted with

Table 7. Crystal Data for New Compounds

	2a	2d· $\frac{1}{2}$ CH <sub>2</sub> Cl <sub>2</sub>	4d	5
mol formula	C <sub>28</sub> H <sub>35</sub> FeMo <sub>2</sub> O <sub>5</sub> P <sub>3</sub>	C <sub>59</sub> H <sub>72</sub> Cl <sub>2</sub> Mo <sub>4</sub> O <sub>12</sub> P <sub>6</sub> W <sub>2</sub>	C <sub>29</sub> H <sub>32</sub> Mo <sub>2</sub> O <sub>7</sub> P <sub>2</sub> W	C <sub>33</sub> H <sub>39</sub> MnMo <sub>2</sub> O <sub>5</sub> P <sub>2</sub>
mol wt	792.20	1981.35	930.22	824.4
cryst syst	monoclinic	triclinic	triclinic	monoclinic
space group	<i>P</i> 2 <sub>1</sub> / <i>c</i>	$\bar{P}1$	$\bar{P}1$	<i>P</i> 2 <sub>1</sub> / <i>c</i>
radiation ( $\lambda$ ), Å	1.54184	1.54184	1.54184	1.54184
<i>a</i> , Å	9.9099(2)	11.458(5)	10.4478(8)	10.9898(3)
<i>b</i> , Å	23.5511(5)	18.270(5)	11.2943(12)	15.1118(4)
<i>c</i> , Å	15.7915(4)	18.747(5)	14.2992(17)	19.6212(9)
$\alpha$ , deg	90	111.258(5)	71.451(11)	90
$\beta$ , deg	116.591(2)	99.502(5)	88.166(8)	100.840(4)
$\gamma$ , deg	90	106.801(5)	83.909(8)	90
<i>V</i> , Å <sup>3</sup>	3295.7(1)	3337.3(19)	1590.6(3)	3200.5(2)
<i>Z</i>	4	2	2	4
calcd density, g cm <sup>-3</sup>	1.597	1.972	1.942	1.711
abs coeff, mm <sup>-1</sup>	11.275	14.728	14.21	10.757
temperature, K	100(2)	124(3)	123(2)	123(2)
$\theta$ range, deg	8.81–69.60	2.81–74.55	3.26–74.83	3.72–69.34
index ranges ( <i>h</i> ; <i>k</i> ; <i>l</i> )	–11, 11; –28, 28; –19, 18	–14, 14; –22, 22; –23, 23	–12, 9; –13, 13; –16, 17	–13, 13; –13, 17; –23, 22
no. of reflns collected	17884	60753	12329	14021
no. of indep reflns ( <i>R</i> <sub>int</sub> )	6059 (0.0296)	13398 (0.0451)	6180 (0.0951)	5857 (0.0546)
reflns with <i>I</i> > 2 $\sigma$ ( <i>I</i> )	5408	11684	3627	4604
<i>R</i> indexes [data with <i>I</i> > 2 $\sigma$ ( <i>I</i> )] <sup>a</sup>	<i>R</i> <sub>1</sub> = 0.0303, <i>wR</i> <sub>2</sub> = 0.0863 <sup>b</sup>	<i>R</i> <sub>1</sub> = 0.0328, <i>wR</i> <sub>2</sub> = 0.0802 <sup>c</sup>	<i>R</i> <sub>1</sub> = 0.0695, <i>wR</i> <sub>2</sub> = 0.1673 <sup>d</sup>	<i>R</i> <sub>1</sub> = 0.0523, <i>wR</i> <sub>2</sub> = 0.1292 <sup>e</sup>
<i>R</i> indexes (all data) <sup>a</sup>	<i>R</i> <sub>1</sub> = 0.0345, <i>wR</i> <sub>2</sub> = 0.0888 <sup>b</sup>	<i>R</i> <sub>1</sub> = 0.0399, <i>wR</i> <sub>2</sub> = 0.0855 <sup>c</sup>	<i>R</i> <sub>1</sub> = 0.1221, <i>wR</i> <sub>2</sub> = 0.2121 <sup>d</sup>	<i>R</i> <sub>1</sub> = 0.0686, <i>wR</i> <sub>2</sub> = 0.1424 <sup>e</sup>
GO <sub>F</sub>	1.074	1.045	0.954	1.013
no. of restraints/params	0/353	0/758	12/354	0/389
$\Delta\rho$ (max), $\Delta\rho$ (min), e Å <sup>-3</sup>	0.941, –0.654	1.279, –1.428	1.520, –1.689	2.546, –1.488

<sup>a</sup>*R*<sub>1</sub> =  $\sum ||F_o| - |F_c|| / \sum |F_o|$ . *wR*<sub>2</sub> =  $[\sum w(|F_o|^2 - |F_c|^2)^2 / \sum w|F_o|^2]^{1/2}$ . *w* =  $1/[\sigma^2(F_o^2) + (aP)^2 + bP]$ , where *P* =  $(F_o^2 + 2F_c^2)/3$ . <sup>b</sup>*a* = 0.0504 and *b* = 2.6898. <sup>c</sup>*a* = 0.0403 and *b* = 8.5689. <sup>d</sup>*a* = 0.0899 and *b* = 0.0000. <sup>e</sup>*a* = 0.0841 and *b* = 0.0000.

dichloromethane/petroleum ether (1:4), and the extract chromatographed through alumina at 288 K. Elution with the same solvent mixture gave a yellow fraction, yielding, after removal of solvents, compound **4d** as a yellow solid (0.020 g, 69%). Crystals suitable for X-ray diffraction analysis were obtained by the slow diffusion of a layer of petroleum ether into a concentrated toluene solution of the complex at 253 K. Anal. Calcd for C<sub>29</sub>H<sub>32</sub>Mo<sub>2</sub>O<sub>7</sub>P<sub>2</sub>W: C, 37.44; H, 3.47. Found: C, 37.11; H, 3.42. <sup>1</sup>H NMR:  $\delta$  5.86 (s, 10H, Cp), 2.49 (d, br, *J*<sub>PH</sub> = 13, 2H, Cy), 2.09 (m, 2H, Cy), 2.0–1.0 (m, 18H, Cy). <sup>13</sup>C{<sup>1</sup>H} NMR (100.61 MHz):  $\delta$  218.1 (t, *J*<sub>CP</sub> = 12, MoCO), 212.6 [d, *J*<sub>CP</sub> = 15, WCO(ax)], 198.5 [d, *J*<sub>CP</sub> = 3, WCO(eq)], 91.5 (s, Cp), 45.6 [d, *J*<sub>CP</sub> = 2, C1(Cy)], 35.8 [d, *J*<sub>CP</sub> = 2, C2(Cy)], 33.5 [s, C2(Cy)], 28.27 [d, *J*<sub>CP</sub> = 11, C3(Cy)], 28.26 [d, *J*<sub>CP</sub> = 13, C3(Cy)], 26.4 [s, C4(Cy)].

**Preparation of [MnMo<sub>2</sub>Cp<sub>2</sub>Cp'(μ<sub>3</sub>-P)(μ-PCy<sub>2</sub>)(CO)<sub>5</sub>] (5).** A dichloromethane solution (4 mL) of compound **4b** (0.020 g, 0.025 mmol) was placed in a bulb equipped with a Young's valve. The bulb was cooled at 77 K, evacuated under vacuum, and then refilled with CO. The valve was then closed, and the solution was allowed to reach room temperature and further stirred for 10 min to give an orange solution mainly containing compound **5**, which was obtained as a red-orange solid upon removal of solvents. This compound undergoes spontaneous decarbonylation to give back compound **4b** in the absence of a CO atmosphere, and therefore it was not isolated as a pure solid in bulk. However, a few crystals of **5** suitable for X-ray analysis were grown by the slow diffusion of layers of petroleum ether and diethyl ether into a concentrated toluene solution of the complex (contaminated with **4b**) at 253 K. IR [ $\nu$ (CO), Nujol]: 1963 (m, sh), 1953 (s), 1910 (m), 1902 (m, sh), 1894 (vs), 1847 (s). <sup>1</sup>H NMR:  $\delta$  5.28, 5.19 (2s, 2 × 5H, Cp), 4.79 (m, 2H, C<sub>5</sub>H<sub>4</sub>), 4.67, 4.63 (2m, 2 × 1H, C<sub>5</sub>H<sub>4</sub>), 1.96 (s, 3H, Me), 2.50–0.80 (m, 22H, Cy). <sup>1</sup>H NMR (400.13 MHz, 223 K):  $\delta$  5.30, 5.22 (2s, 2 × 5H, Cp), 4.85 (m, 2H, C<sub>5</sub>H<sub>4</sub>), 4.72, 4.61 (2m, 2 × 1H, C<sub>5</sub>H<sub>4</sub>), 1.97 (s, 3H, Me), 2.50–0.80 (m, 22H, Cy). <sup>31</sup>P{<sup>1</sup>H} NMR:  $\delta$  951.0 (d, *J*<sub>PP</sub> = 11, μ<sub>3</sub>-P), 223.2 (s, *J*<sub>PP</sub> = 11, μ-PCy<sub>2</sub>). <sup>31</sup>P{<sup>1</sup>H} NMR (161.98 MHz, 223 K):  $\delta$  942.6 (s, μ<sub>3</sub>-P), 220.9 (s, μ-PCy<sub>2</sub>). <sup>13</sup>C{<sup>1</sup>H} NMR (100.61 MHz, 223 K):  $\delta$  93.5, 89.9

(2s, Cp), 86.8, 86.1, 85.8, 83.5 [4s, CH(C<sub>5</sub>H<sub>4</sub>)], 36.7 [d, *J*<sub>CP</sub> = 15, C1(Cy)], 35.4, 34.0, 33.6 [3s, C2(Cy)], 28.9 [d, *J*<sub>CP</sub> = 10, C3(Cy)], 28.5 [d, *J*<sub>CP</sub> = 9, C3(Cy)], 27.7 [s, C2(Cy)], 27.5, 27.4 [2d, *J*<sub>CP</sub> = 15, C3(Cy)], 26.6, 26.2 [2s, C4(Cy)], 14.2 (s, Me). Resonances due to carbonyl ligands and the C1 atom of the C<sub>5</sub>H<sub>4</sub> ring could not be identified in this spectrum, whereas the missing C1(Cy) resonance most likely is obscured by that of the solvent.

**Preparation of [Mo<sub>2</sub>WCp<sub>2</sub>(μ<sub>3</sub>-P)(μ-PCy<sub>2</sub>)(μ-CO)(CO)<sub>5</sub>] (6).** A THF solution (7 mL) of compound **1** (0.030 g, 0.046 mmol) was mixed with a THF solution of [W(CO)<sub>5</sub>(THF)], prepared in situ from 0.017 g (0.048 mmol) of [W(CO)<sub>6</sub>], in a Schlenk tube equipped with a Young's valve, and the mixture was stirred for 50 min at room temperature to give a brown-orange solution. Solvent was then removed under vacuum, and the residue was dissolved in toluene (7 mL) and refluxed for 3 h. After removal of solvents, the residue was extracted with dichloromethane/petroleum ether (1:2) and the extract chromatographed through alumina. Elution with dichloromethane/petroleum ether (1:5) gave first a yellow fraction containing small amounts of **4d** and then an orange fraction, yielding, after removal of solvents, compound **6** as a red solid (0.023 g, 55%). Anal. Calcd for C<sub>28</sub>H<sub>32</sub>Mo<sub>2</sub>O<sub>6</sub>P<sub>2</sub>W: C, 37.28; H, 3.58. Found: C, 37.20; H, 3.56. <sup>1</sup>H NMR:  $\delta$  5.95 (s, 10H, Cp), 1.95–0.90 (m, 18H, Cy), 0.59, 0.45 (2m, 2 × 2H, Cy). <sup>31</sup>P{<sup>1</sup>H} NMR:  $\delta$  925.2 (d, *J*<sub>PP</sub> = 30, *J*<sub>PW</sub> = 160, μ<sub>3</sub>-P), 246.0 (d, *J*<sub>PP</sub> = 30, μ-PCy<sub>2</sub>). <sup>13</sup>C{<sup>1</sup>H} NMR (150.91 MHz):  $\delta$  296.8 (s, μ-CO), 206.4 [d, *J*<sub>CP</sub> = 17, WCO(ax)], 197.5 [d, *J*<sub>CP</sub> = 6, *J*<sub>CW</sub> = 127, WCO(eq)], 94.1 (s, Cp), 44.6 [d, *J*<sub>CP</sub> = 16, C1(Cy)], 40.8 [d, *J*<sub>CP</sub> = 19, C1(Cy)], 33.7, 33.1 [2s, C2(Cy)], 27.6, 27.3 [2d, *J*<sub>CP</sub> = 12, C3(Cy)], 26.3, 25.9 [2s, C4(Cy)].

**X-ray Structure Determination for Compounds 2a, 2d, 4d, and 5.** Data collection for these compounds was performed on an Oxford Diffraction Xcalibur Nova single-crystal diffractometer, using Cu K $\alpha$  radiation ( $\lambda$  = 1.5418 Å) at 100 K (**2a**) or 123 K. Images were collected at a 90 mm (**2a**) or 63 mm fixed crystal–detector distance, using the oscillation method, with 1° oscillation and variable exposure time per image (11–16 s for **2a**, 1.5–2 s for **2d**, 5–80 s for **4d**, and



25–60 s for **5**). The data collection strategy was calculated with the program *CrysAlis Pro CCD*.<sup>50</sup> Data reduction and cell refinement were performed with the program *CrysAlis Pro RED*.<sup>50</sup> An empirical absorption correction was applied using the SCALE3 ABSPACK algorithm, as implemented in the program *CrysAlis Pro RED*. Using the program suite *WinGX*,<sup>51</sup> the structures were generally solved by Patterson interpretation and phase expansion using *SHELXL97*,<sup>52</sup> and refined with full-matrix least squares on  $F^2$  using *SHELXL97*, except for **2d**, which was solved with *SIR92*.<sup>53</sup> In general, all of the positional parameters and anisotropic temperature factors of all non-H atoms were refined anisotropically, except for the C atoms involved in disorder, which were refined isotropically to prevent their temperature factors from becoming nonpositive definite, and all H atoms were geometrically placed and refined using a riding model. Compound **2a** was crystallized with a molecule of toluene, found to be disordered, and placed on a symmetry element. This disorder could not be solved; therefore, the *SQUEEZE* procedure,<sup>54</sup> as implemented in *PLATON*,<sup>55</sup> was used. Upon *SQUEEZE* application and convergence, the strongest residual peak ( $0.94 \text{ e \AA}^{-3}$ ) was placed between the Mo2 and P1 atoms. In the case of **2d**, there were two independent molecules of the complex and a molecule of dichloromethane in the asymmetric unit. One of the cyclopentadienyl ligands in each case was disordered over two positions and satisfactorily modeled with occupancies 0.5/0.5 and 0.6/0.4 respectively. In the case of **4d**, one of the carbonyl ligands and one of the cyclopentadienyl groups also were disordered. The cyclopentadienyl group was satisfactorily modeled over two positions with 0.5/0.5 occupancy. However, the disorder in the C2O2 ligand could not be solved; moreover, the corresponding thermal ellipsoids had no chemical sense, so eventually these atoms were refined isotropically with restraints in the Mo2–C2 and C2–O2 distances to get a sensible geometry for this CO group, analogous to that of the other molybdenum-bound carbonyl. Crystallographic data and structure refinement details for all of these compounds are collected in Table 7.

**Computational Details.** Computations were carried out using the *GAUSSIAN03* package,<sup>56</sup> in which the hybrid methods B3LYP and UB3LYP [ $\text{PW}(\text{CO})_5$ ] were applied with the Becke three-parameter exchange functional<sup>57</sup> and the Lee–Yang–Parr correlation functional.<sup>58</sup> An accurate numerical integration grid (99590) was used for all of the calculations via the keyword *Int=Ultrafine*. Effective core potentials and their associated double- $\zeta$  LANL2DZ basis set were used for the metal atoms.<sup>59</sup> The light elements (P, O, C, and H) were described with the 6-31G\* basis set.<sup>60</sup> Geometry optimizations were performed under no symmetry restrictions, using the initial coordinates derived from the X-ray data of **4d** and **5**. Frequency analyses were performed for all stationary points to ensure that a minimum structure with no imaginary frequencies was achieved in each case. Molecular orbitals were visualized using the *MOLEKEL* program,<sup>61</sup> and topological analysis of the electron density was carried out with the *Xaim* routine.<sup>62</sup>

## ■ ASSOCIATED CONTENT

### ■ Supporting Information

CIF file containing full crystallographic data for compounds **2a**, **2d**, **4d**, and **5** (CCDC 1013089–1013092) and a PDF file containing details of DFT calculations of compounds **4d** and **5** and related fragments (atomic coordinates, selected bond lengths and angles, and molecular orbitals). This material is available free of charge via the Internet at <http://pubs.acs.org>.

## ■ AUTHOR INFORMATION

### Corresponding Authors

\*E-mail: [ara\\_12\\_79@hotmail.com](mailto:ara_12_79@hotmail.com).

\*E-mail: [mara@uniovi.es](mailto:mara@uniovi.es).

### Notes

The authors declare no competing financial interest.

## ■ ACKNOWLEDGMENTS

We thank the DGI of Spain for financial support (Projects CTQ2009-09444 and CTQ2012-33187) and the CMC of Universidad de Oviedo for access to computing facilities. A.R. thanks the CSIC for a JAE-Doc contract, cofunded by the European Social Fund.

## ■ REFERENCES

- (1) (a) Alvarez, M. A.; García, M. E.; García-Vivó, D.; Ramos, A.; Ruiz, M. A. *Inorg. Chem.* **2011**, *50*, 2064. (b) Alvarez, M. A.; García, M. E.; García-Vivó, D.; Ramos, A.; Ruiz, M. A. *Inorg. Chem.* **2012**, *51*, 11061.
- (2) Weber, L. *Chem. Rev.* **1992**, *82*, 1839.
- (3) (a) Weber, L.; Meine, G.; Boese, R.; Bläser, D. *Chem. Ber.* **1988**, *121*, 853. (b) Weber, L.; Meine, G. *Chem. Ber.* **1987**, *120*, 457.
- (4) (a) Weber, L.; Schumann, L.; Stammer, H.-G.; Neumann, B. J. *Organomet. Chem.* **1993**, *443*, 175. (b) A similar coordination mode is displayed at the phosphine–diphosphorus-bridged CoPt complex [ $\text{CoPt}(\mu\text{-P}_2\text{PPh}_2\text{CH}_2\text{PPh}_2)_2(\text{PPh}_3)_2$ ] $\text{BF}_4$ . See: Caporali, M.; Barbaro, P.; Gonsalvi, L.; Ienco, A.; Yakhvarov, D.; Peruzzini, M. *Angew. Chem., Int. Ed.* **2008**, *47*, 3766.
- (5) Feske, D.; Queisser, J.; Schottmüller, H. Z. *Anorg. Allg. Chem.* **1996**, *622*, 1731.
- (6) Weber, L.; Schumann, H. *Chem. Ber.* **1991**, *124*, 265.
- (7) Scherer, O. J.; Ehses, M.; Wolmershäuser, G. *Angew. Chem., Int. Ed.* **1998**, *37*, 507.
- (8) (a) Caporali, M.; Gonsalvi, L.; Rossin, A.; Peruzzini, M. *Chem. Rev.* **2010**, *110*, 4178. (b) Cossairt, B. M.; Piro, N. A.; Cummins, C. C. *Chem. Rev.* **2010**, *110*, 4164.
- (9) Alvarez, M. A.; García, M. E.; Lozano, R.; Ramos, A.; Ruiz, M. A., results to be published.
- (10) Alvarez, M. A.; García, M. E.; García-Vivó, D.; Lozano, R.; Ramos, A.; Ruiz, M. A. *Inorg. Chem.* **2013**, *52*, 9005.
- (11) Alvarez, C. M.; Alvarez, M. A.; García, M. E.; Ramos, A.; Ruiz, M. A.; Graiff, C.; Tiripicchio, A. *Organometallics* **2007**, *26*, 321.
- (12) Cordero, B.; Gómez, V.; Platero-Prats, A. E.; Revés, M.; Echeverría, J.; Cremades, E.; Barragán, F.; Alvarez, S. *Dalton Trans.* **2008**, 2832.
- (13) Scheer, M.; Leiner, E.; Kramkowski, P.; Schiffer, M.; Baum, G. *Chem.—Eur. J.* **1998**, *4*, 1917.
- (14) Scheer, M.; Himmel, D.; Kuntz, C.; Zhan, S.; Leiner, E. *Chem.—Eur. J.* **2008**, *14*, 9020.
- (15) (a) Cotton, F. A.; Frenz, B. A.; White, A. J. *Inorg. Chem.* **1974**, *13*, 1407. (b) Klasen, C.; Lorenz, I. P.; Schmid, S.; Beuter, G. J. *Organomet. Chem.* **1992**, *428*, 363. (c) Alvarez, C. M.; Galán, B.; García, M. E.; Riera, V.; Ruiz, M. A.; Vaissermann, J. *Organometallics* **2003**, *22*, 5504. (d) Alvarez, M. A.; García, M. E.; García-Vivó, D.; Ramos, A.; Ruiz, M. A. *Inorg. Chem.* **2012**, *51*, 3698.
- (16) Alvarez, C. M.; Alvarez, M. A.; García, M. E.; González, R.; Ramos, A.; Ruiz, M. A. *Inorg. Chem.* **2011**, *50*, 10937.
- (17) Bridgeman, A. J.; Mays, M. J.; Woods, A. D. *Organometallics* **2001**, *20*, 2076.
- (18) Braterman, P. S. *Metal Carbonyl Spectra*; Academic Press: London, U.K., 1975.
- (19) (a) García, M. E.; García-Vivó, D.; Ruiz, M. A. *Organometallics* **2009**, *28*, 4385. (b) Alvarez, M. A.; García, M. E.; Martínez, M. E.; Ruiz, M. A. *Organometallics* **2010**, *29*, 904.
- (20) Mays, M. J.; Raithby, P. R.; Sarveswaran, K.; Solan, G. A. *Dalton Trans.* **2002**, 1671.
- (21) Huttner, G.; Knoll, K. *Angew. Chem., Int. Ed. Engl.* **1987**, *26*, 743.
- (22) Carty, A. J.; MacLaughlin, S. A.; Nucciarone, D. In *Phosphorus-31 NMR Spectroscopy in Stereochemical Analysis*; Verkade, J. G., Quin, L. D., Eds.; VCH: Deerfield Beach, FL, 1987; Chapter 16.
- (23) Davies, J. E.; Klunduk, M. C.; Mays, M. J.; Raithby, P. R.; Shields, G. P.; Tompkin, P. K. *J. Chem. Soc., Dalton Trans.* **1997**, 715.
- (24) Adatia, T.; McPartlin, M.; Mays, M. J.; Morris, M. J.; Raithby, P. R. *J. Chem. Soc., Dalton Trans.* **1989**, 1555.

- (25) (a) García, M. E.; Ramos, A.; Ruiz, M. A.; Lanfranchi, M.; Marchiò, L. *Organometallics* **2007**, *26*, 6197. (b) Alvarez, M. A.; García, M. E.; García-Vivó, D.; Martínez, M. E.; Ruiz, M. A. *Organometallics* **2011**, *30*, 2189. (c) García, M. E.; García-Vivó, D.; Ruiz, M. A.; Alvarez, S.; Aullón, G. *Organometallics* **2007**, *26*, 5912. (d) Alvarez, M. A.; García, M. E.; Ramos, A.; Ruiz, M. A. *Organometallics* **2007**, *26*, 1461.
- (26) Arif, A. M.; Cowley, A. H.; Norman, N. C.; Orpen, A. G.; Pakulski, M. *Organometallics* **1988**, *7*, 309.
- (27) García, M. E.; Riera, V.; Ruiz, M. A.; Sáez, D.; Vaissermann, J.; Jeffery, J. C. *J. Am. Chem. Soc.* **2002**, *124*, 14304.
- (28) Amor, I.; García, M. E.; Ruiz, M. A.; Sáez, D.; Hamidov, H.; Jeffery, J. C. *Organometallics* **2006**, *25*, 4857.
- (29) Huttner, G.; Evertz, K. *Acc. Chem. Res.* **1986**, *19*, 406.
- (30) Alvarez, M. A.; Amor, I.; García, M. E.; García-Vivó, D.; Ruiz, M. A.; Hamidov, H.; Jeffery, J. C. *Inorg. Chim. Acta* **2014**, in press (DOI: <http://dx.doi.org/10.1016/j.ica.2014.04.043>).
- (31) Bode, M.; Schnakenburg, G.; Daniels, J.; Marinetti, A.; Streubel, R. *Organometallics* **2010**, *29*, 656.
- (32) Ulbaev, T. S.; Mardashev, Y. S.; Koroteev, M. P.; Khrustalev, V. N.; Antipin, M. Y. *Zh. Strukt. Khim.* **2005**, *46*, 924.
- (33) (a) Kramkowski, P.; Baum, G.; Radius, U.; Kaupp, M.; Scheer, M. *Chem.—Eur. J.* **1999**, *5*, 2890. (b) Scheer, M.; Kramkowski, P.; Schuster, K. *Organometallics* **1999**, *18*, 2874.
- (34) Groer, T.; Scheer, M. *Z. Anorg. Allg. Chem.* **2000**, *626*, 1211.
- (35) Bader, R. F. W. *Atoms in molecules—A Quantum Theory*; Oxford University Press: Oxford, U.K., 1990.
- (36) Alvarez, M. A.; Amor, I.; García, M. E.; García-Vivó, D.; Ruiz, M. A.; Suárez, J. *Organometallics* **2010**, *29*, 4384.
- (37) (a) Hoffmann, R. *Angew. Chem., Int. Ed. Engl.* **1982**, *21*, 711. (b) Stone, F. G. A. *Angew. Chem., Int. Ed. Engl.* **1984**, *23*, 89.
- (38) Jean, Y. *Molecular Orbitals of Transition Metal Complexes*; Oxford University Press: Oxford, U.K., 2003, Chapter 5.
- (39) García, M. E.; Riera, V.; Ruiz, M. A.; Rueda, M. T.; Sáez, D. *Organometallics* **2002**, *21*, 5515.
- (40) (a) Giffin, N. A.; Masuda, J. D. *Coord. Chem. Rev.* **2011**, *255*, 1342. (b) Scheer, M.; Balazs, G.; Seitz, A. *Chem. Rev.* **2010**, *110*, 4236.
- (41) (a) Alvarez, M. A.; García, M. E.; Ramos, A.; Ruiz, M. A. *J. Organomet. Chem.* **2009**, *694*, 3864. (b) Alvarez, M. A.; García, M. E.; Ramos, A.; Ruiz, M. A.; Lanfranchi, M.; Tiripicchio, A. *Organometallics* **2007**, *26*, 5454.
- (42) (a) García, M. E.; García-Vivó, D.; Ruiz, M. A.; Alvarez, S.; Aullón, G. *Organometallics* **2007**, *26*, 4930. (b) Alvarez, M. A.; García, M. E.; García-Vivó, D.; Menéndez, S.; Ruiz, M. A. *Organometallics* **2013**, *32*, 218.
- (43) Reginato, N.; McGlinchey, M. J. *Organometallics* **2001**, *20*, 4147.
- (44) Huttner, G.; Weber, U.; Sigwarth, B.; Scheidsteger, O.; Lang, H.; Zsolnai, L. *J. Organomet. Chem.* **1985**, *282*, 331.
- (45) A general trend established for  ${}^2J_{XY}$  in complexes of the type  $[MCpXYL_2]$  is that it increases algebraically with the X–M–Y angle, with absolute values in the order  $|J_{cis}| > |J_{trans}|$ . For instance, see: Jameson, C. J. In *Phosphorus-31 NMR Spectroscopy in Stereochemical Analysis*; Verkade, J. G., Quin, L. D., Eds.; VCH: Deerfield Beach, FL, 1987; Chapter 6.
- (46) Armarego, W. L. F.; Chai, C. *Purification of Laboratory Chemicals*, 5th ed.; Butterworth-Heinemann: Oxford, U.K., 2003.
- (47) Johnson, E. C.; Meyer, T. J.; Winterton, N. *Inorg. Chem.* **1971**, *10*, 218.
- (48) Hermann, W. W. *Angew. Chem.* **1974**, *86*, 345.
- (49) (a) Gibson, V. C.; Long, N. J.; Long, R. J.; White, A. J. P.; Williams, C. K.; Williams, D. J.; Grigiotti, E.; Zanello, P. *Organometallics* **2004**, *23*, 957. (b) Sellman, D.; Brandl, A.; Endell, R. *J. Organomet. Chem.* **1975**, *97*, 229.
- (50) *CrysAlis Pro*; Oxford Diffraction Ltd.: Oxford, U.K., 2006.
- (51) Farrugia, L. J. *J. Appl. Crystallogr.* **1999**, *32*, 837.
- (52) Sheldrick, G. M. *Acta Crystallogr.* **2008**, *A64*, 112.
- (53) Altomare, A.; Casciarano, G.; Giacovazzo, C.; Guagliardi, A.; Burla, M. C.; Polidori, G.; Camalli, M. *J. Appl. Crystallogr.* **1994**, *27*, 435.
- (54) Van der Sluis, P.; Spek, A. L. *Acta Crystallogr.* **1990**, *A46*, 194.
- (55) Spek, A. L. *PLATON, A Multipurpose Crystallographic Tool*; Utrecht University: Utrecht, The Netherlands, 2010.
- (56) Frisch, M. J.; Trucks, G. W.; Schlegel, H. B.; Scuseria, G. E.; Robb, M. A.; Cheeseman, J. R.; Montgomery, J. A., Jr.; Vreven, T.; Kudin, K. N.; Burant, J. C.; Millam, J. M.; Iyengar, S. S.; Tomasi, J.; Barone, V.; Mennucci, B.; Cossi, M.; Scalmani, G.; Rega, N.; Petersson, G. A.; Nakatsuji, H.; Hada, M.; Ehara, M.; Toyota, K.; Fukuda, R.; Hasegawa, J.; Ishida, M.; Nakajima, T.; Honda, Y.; Kitao, O.; Nakai, H.; Klene, M.; Li, X.; Knox, J. E.; Hratchian, H. P.; Cross, J. B.; Bakken, V.; Adamo, C.; Jaramillo, J.; Gomperts, R.; Stratmann, R. E.; Yazyev, O.; Austin, A. J.; Cammi, R.; Pomelli, C.; Ochterski, J. W.; Ayala, P. Y.; Morokuma, K.; Voth, G. A.; Salvador, P.; Dannenberg, J. J.; Zakrzewski, V. G.; Dapprich, S.; Daniels, A. D.; Strain, M. C.; Farkas, O.; Malick, D. K.; Rabuck, A. D.; Raghavachari, K.; Foresman, J. B.; Ortiz, J. V.; Cui, Q.; Baboul, A. G.; Clifford, S.; Cioslowski, J.; Stefanov, B. B.; Liu, G.; Liashenko, A.; Piskorz, P.; Komaromi, I.; Martin, R. L.; Fox, D. J.; Keith, T.; Al-Laham, M. A.; Peng, C. Y.; Nanayakkara, A.; Challacombe, M.; Gill, P. M. W.; Johnson, B.; Chen, W.; Wong, M. W.; Gonzalez, C.; Pople, J. A. *GAUSSIAN03*, revision B.02; Gaussian, Inc.: Wallingford, CT, 2004.
- (57) Becke, A. D. *J. Chem. Phys.* **1993**, *98*, 5648.
- (58) Lee, C.; Yang, W.; Parr, R. G. *Phys. Rev. B* **1988**, *37*, 785.
- (59) Hay, P. J.; Wadt, W. R. *J. Chem. Phys.* **1985**, *82*, 299.
- (60) (a) Hariharan, P. C.; Pople, J. A. *Theor. Chim. Acta* **1973**, *28*, 213. (b) Petersson, G. A.; Al-Laham, M. A. *J. Chem. Phys.* **1991**, *94*, 6081. (c) Petersson, G. A.; Bennett, A.; Tensfeldt, T. G.; Al-Laham, M. A.; Shirley, W. A.; Mantzaris, J. *J. Chem. Phys.* **1988**, *89*, 2193.
- (61) MOLEKEL: An Interactive Molecular Graphics Tool: Portmann, S.; Lüthi, H. P. *CHIMIA Int. J.* **2000**, *54*, 766.
- (62) Ortiz, J. C.; Bo, C. *Xaim*; Departamento de Química Física e Inorgánica, Universidad Rovira i Virgili: Tarragona, Spain, 1998.